Monthly Notices
of the
ROYAL ASTRONOMICAL SOCIETY

Mon. Not. R. Astron. Soc. **414,** 167–183 (2011) doi:10.1111/j.1365-2966.2011.18363.x

# SN 2008gz – most likely a normal Type IIP event

Rupak Roy,[1⋆] Brijesh Kumar,[1] Alexander S. Moskvitin,[2] Stefano Benetti,[3] Timur A. Fatkhullin,[2] Brajesh Kumar,[1,4] Kuntal Misra,[5,6] Filomena Bufano,[3] Ralph Martin,[7] Vladimir V. Sokolov,[2] S. B. Pandey,[1,8] H. C. Chandola[9] and Ram Sagar[1]

[1]*Aryabhatta Research Institute of Observational Sciences (ARIES), Manora Peak, Nainital 263129, India*
[2]*Special Astrophysical Observatory, Nizhnij Arkhyz, Karachaevo-Cherkesia 369167, Russia*
[3]*Istituto Nazionale di Astrofisica, Osservatorio Astronomico di Padova, Vicolo dell'Osservatorio 5, 35122 Padova, Italy*
[4]*Institut d'Astrophysique et de Géophysique, Université de Liège, Allée du 6 Août 17, Bât B5c, 4000 Liège, Belgium*
[5]*Space Telescope Science Institute, 3700 San Martin Drive, Baltimore, MD 21218, USA*
[6]*Inter University Center for Astronomy and Astrophysics, Post Bag 4, Ganeshkhind, Pune 411007, India*
[7]*Perth Observatory, 337 Walnut Road, Bickley 6076, Perth, Australia*
[8]*Randall Laboratory of Physics, Univ. Michigan, 450 Church St., Ann Arbor, MI 48109-1040, USA*
[9]*Department of Physics, Kumaun University, Nainital, India*

Accepted 2011 January 13. Received 2011 January 13; in original form 2010 October 25

**ABSTRACT**

We present *BVRI* photometric and low-resolution spectroscopic investigation of the Type II core-collapse supernova (SN) 2008gz, which occurred in a star-forming arm and within a half-light radius (solar metallicity region) of the nearby spiral galaxy NGC 3672. The SN event was detected late, and a detailed investigation of its light curves and spectra spanning 200 d suggest that it is an event of Type IIP similar to the archetypal SNe 2004et and 1999em. However, in contrast to other events of its class, SN 2008gz exhibits a rarely observed *V* magnitude drop of 1.5 over the period of a month during the plateau to nebular phase. Using an $A_V$ of 0.21 mag as a lower limit and a distance of 25.5 Mpc, we estimate a synthesized $^{56}$Ni mass of $0.05 \pm 0.01\,M_\odot$, a mid-plateau $M_V$ of $-16.6 \pm 0.2$ mag and a total radiant energy of $\sim 10^{49}$ erg. The photospheric velocity is observed to be higher than observed for SN 2004et at similar epochs, indicating that the explosion energy was comparable to or higher than that of SN 2004et. A similar trend was also seen for the expansion velocity of H envelopes. By comparing the properties of SN 2008gz with other well-studied events, as well as by using a recent simulation of pre-SN models by Dessart, Livne & Waldman, we infer an explosion energy range of 2–3 $\times$ $10^{51}$ erg, and this coupled with the observed width of the forbidden [O I] 6300–6364 Å line at 275 d after the explosion gives an upper limit for the main-sequence (non-rotating, solar metallicity) progenitor mass of $17\,M_\odot$. Our narrow-band H$\alpha$ observation, taken nearly 560 d after the explosion, and the presence of an emission kink at zero velocity in the Doppler-corrected spectra of SN indicate that the event took place in a low-luminosity star-forming H II region.

**Key words:** supernovae: general – supernovae: individual: SN 2008gz – galaxies: distances and redshifts – galaxies: individual: NGC 3672.

## 1 INTRODUCTION

Core-collapse supernovae occur in late-type galaxies and their locations are usually associated with regions of high stellar surface brightness or recent/ongoing star formation, suggesting that they represent the end stages of massive stars ($M > 8$–$10\,M_\odot$: Anderson & James 2009; Hakobyan et al. 2009). Observationally, these events are classified into H-rich Type II SNe, which show prominent H lines in their optical spectra, and H-deficient Type Ib/c SNe, which do not show traces of H lines. Type Ic events lack He lines as well. Type II SNe constitute about 70 per cent of all core-collapse SNe (Cappellaro, Evans & Turatto 1999; Smith et al. 2009) and their light curves and spectra differ significantly. In Type IIP, the optical light remains constant for about 100 d (called the plateau phase) and then decays exponentially. The spectra of Type IIP events show features

⋆E-mail: roy@aries.res.in; rupakroy1980@gmail.com

of strong P Cygni profiles, while in Type IIL SNe a linear decline in the optical light and strong emission lines are observed. Type IIn events show narrow emission lines (Filippenko 1997; Smartt et al. 2009).

Theoretically, the explosion mechanism consists of the collapse of the progenitor star's Fe-core, formation of a shock wave, ejection of the stellar envelope and formation of a neutron star or a black hole. The shock wave generated through the reversal of core-collapse breaks out of the stellar surface of the progenitor as hot fireball flashes in the X-ray and ultraviolet, continuing for from a few seconds to a few days. In H-rich events, the shock-heated expanding stellar envelope cools down by recombination of H and sustains the plateau phase of IIP SNe, while the post-maxima/plateau light curves are powered by the radioactive decay of $^{56}$Co into $^{56}$Fe. Though the explosion mechanism is similar to the one for these events, they differ largely in energetics, e.g. IIP SNe are observed to form a sequence from low-luminosity, low-velocity, Ni-poor events to bright, high-velocity, Ni-rich objects (Hamuy 2003). Thus, a detailed investigation of individual core-collapse events is important for understanding the nature and environment of progenitors. They generally probe star-formation processes and galactic chemical evolution and constrain stellar evolutionary models (Heger et al. 2003; Smartt 2009; Habergham, Anderson & James 2010). Type IIP SNe also turn out to be good standardizable candles (Hamuy & Pinto 2002; Poznanski et al. 2009; Olivares et al. 2010).

The SN 2008gz event was discovered on 2008 November 5.83 UT by Koichi Itagaki using a 0.6-m telescope in the spiral galaxy NGC 3672 at an unfiltered magnitude of about 16.2. On November 7.84 and 8.84 UT, an independent discovery of this new transient was reported by R. Martin from Perth Observatory as a part of 'Perth Automated Supernova Search Program' using the 0.6-m Lowell Telescope. The red magnitude of this new object was about 15.5 (Nakano & Martin 2008). On November 11.25 UT, Benetti, Boschin & Harutyunyan (2008) took the first spectra of this event with the 3.5 m Telescopio Nazionale Galileo (TNG) (+ DOLORES; range 340–800 nm, resolution 1.0 nm) and showed that it is a Type II supernova event, and by using the GELATO tool (Harutyunyan et al. 2008) they found that the spectrum of SN 2008gz best resembles that of the II-peculiar event SN 1998A, taken at 62 d after explosion (Pastorello et al. 2005). Assuming the recession velocity of the host galaxy $\sim$1862 km s$^{-1}$, they found that the expansion velocity of the hydrogen layer was about 6600 km s$^{-1}$. An independent regular *BVRI* CCD photometric monitoring of SN 2008gz has been carried out since 2008 November 10 using the 1-m Sampurnanand Telescope at Nainital, India. We also collected spectra in the optical (0.4–0.9 μm) with the 2-m IUCAA Girawali Observatory (IGO) telescope, India, 3.6-m New Technology Telescope (NTT), Chile, 6-m Large Altazimuth Telescope (BTA), Russia and 3.6 m TNG located in the Canary Islands, Spain.

In this work, we present the results of optical photometric and low-resolution spectroscopic investigation of SN 2008gz. We adopt the time of explosion as 2009 August 20.0 or JD 245 4694.0, having an uncertainty of a few days (see Section 2.2 for details). Hence the times of post/pre-explosion are rounded off to the nearest day and they are referred to with + and − signs respectively. The basic properties of SN 2008gz and its host galaxy NGC 3672 are given in Table 1.

The remainder of this paper is organized as follows. Sections 2 and 3 present photometric and spectroscopic observations and a brief description of light curves and spectra. In Section 4 we study the evolution of some important line profiles, whereas in Section 5 the velocity of the photosphere and the H ejecta is estimated using the SYNOW code (Branch, Baron & Jeffery 2001; Branch et al. 2002; Baron et al. 2005), which describes spectroscopic observations. Distance, extinction and the evolution of colour and bolometric luminosity are studied in Sections 6 and 7 respectively. The amount of synthesized $^{56}$Ni mass, environment and energetics of the progenitor are estimated and discussed in Section 8. We also made a comparative study of this event with other Type IIP SNe in Section 9. Finally, a summary is presented in Section 10.

**Table 1.** Properties of the host galaxy NGC 3672 and SN 2008gz.

| Parameters | Value | Ref.[a] |
|---|---|---|
| **NGC 3672** | | |
| Type | SAc | 1 |
| RA (J2000) | $\alpha = 11^{\rm h}25^{\rm m}2\overset{\rm s}{.}48$ | 1 |
| Dec. (J2000) | $\delta = -09^\circ47'43\overset{''}{.}0$ | 1 |
| Abs. Magnitude | $M_B = -20.59$ mag | 1 |
| Distance | $D = 25.5 \pm 2.4$ Mpc | Section 6 |
| Scale | $1'' \sim 123$ pc, $1' \sim 7.4$ kpc | |
| Distance modulus | $\mu = 32.03 \pm 0.21$ | |
| Apparent radius | $r_{25} = 1\overset{'}{.}4$ ($\sim$10.4 kpc) | 1 |
| Inclination angle | $\Theta_{\rm inc} = 56\overset{\circ}{.}2$ | 1 |
| Position angle | $\Theta_{\rm maj} = 6\overset{\circ}{.}5$ | 1 |
| Heliocentric Velocity | $cz_{\rm helio} = 1864 \pm 19$ km s$^{-1}$ | 1 |
| **SN 2008gz** | | |
| RA (J2000) | $\alpha = 11^{\rm h}25^{\rm m}3\overset{\rm s}{.}24$ | 2 |
| Dec. (J2000) | $\delta = -09^\circ47'51\overset{''}{.}0$ | 2 |
| Location | 13″ E, 7″ S | 2 |
| Deprojected radius | $r_{\rm SN} = 23\overset{''}{.}37$ ($\sim$2.81 kpc) | Section 8.2 |
| Explosion epoch (UT) | 20.0 August 2008 (JD 2454694.0) | Section 2.2 |
| Discovery date (UT) | 5.83 November 2008 | 2 |

[a](1) HyperLEDA: http://leda.univ-lyon1.fr; (2) Nakano & Martin (2008).

## 2 BROAD-BAND PHOTOMETRY

### 2.1 *BVRI* data

Initial pre-SN images (−403 d) of the host galaxy NGC 3672 in *VRI* bands were obtained from Perth Observatory as part of a supernova search programme for another Type Ia SN 2007bm, which occurred in the same galaxy. Images were taken with a 512 × 512 CCD camera mounted on the 0.6-m Lowell Telescope, covering around 5 × 5 arcmin$^2$ on the sky. The full width at half-maximum (FWHM) seeing was about 2.5 arcsec.

SN 2008gz was observed at different epochs from different observatories around the world. The major part of the monitoring was carried out in Johnson *BV* and Cousins *RI* bands at the 1-m Sampurnanand Telescope (ST)[1] at the Aryabhatta Research Institute of Observational Sciences (ARIES), Nainital, India. SN 2008gz was observed during 2008 November 10 (+87 d) to 2009 May 17 (+275 d). We could not detect the SN in the observations of 2009 November 19 (+462 d) in *B*, 2010 February 13 (+547 d) in *VRI* and

[1] We used a 2048 × 2048 CCD camera having a square pixel of side 24 μm mounted at the $f/13$ Cassegrain focus of the telescope. The plate scale of the CCD chip is 0.38 arcsec per pixel, and the entire chip covers a field of 13 × 13 arcmin$^2$ on the sky. The gain and readout noise of the CCD camera are 10e$^-$ per analogue-to-digital unit and 5.3e$^-$ respectively. All the observations were carried out in the binning mode of 2 × 2 pixel.

**Table 2.** Journal of photometric observation of SN 2008gz. The full table is available online (see Supporting Information).

| UT Date (yy/mm/dd) | JD 245 4000+ | Phase (day) | *B* (s) | *V* (s) | *R* (s) | *I* (s) | Telescope | Seeing (″) | Ellipticity |
|---|---|---|---|---|---|---|---|---|---|
| 2007/07/09 | 290.94 | −403 | – | 240 | 180 | 180 | LT | 2.5 | 0.05 |
| 2008/11/10 | 781.48 | +87 | 2 × 300 | 2 × 300 | 2 × 250 | 2 × 250 | ST | 2.4 | 0.18 |
| – | – | – | – | – | – | – | – | – | – |

2010 February 14 (+548 d) in *BVRI*. In addition to the 1-m ST, observations of SN 2008gz in *BVRI* bands were also obtained on 2009 March 21, 22, 24 and 25, with the IUCAA Faint Object Spectrograph & Camera (IFOSC) mounted on the 2-m IUCAA Girawali Observatory (IGO), IUCAA, India and on 2009 May 17 with the ESO Faint Object Spectrograph and Camera (v.2, EFOSC2) mounted on the 3.6-m NTT, European Southern Observatory (ESO), Chile. The journal of observations is given in Table 2.[2]

Photometric observations included the acquisition of several exposures with exposure time varying from 100–300 s in different filters. Several bias and twilight flat-frames were obtained for the CCD images. Bias-subtraction, flat-fielding, cosmic-ray removal, alignment and determination of mean FWHM and ellipticity in all the object frames were carried out using the standard tasks available in the data reduction software IRAF[3] and DAOPHOT[4] (Stetson 1987, 1992). The FWHM seeing in the *V* band varied from 2–4 arcsec, with a median value of around 2.5 arcsec. About 10 per cent of the images taken at large zenith distance had a highly elongated point-spread function (PSF) (ellipticity $> 0.2$). For the final photometry, we co-added the individual frames to increase the signal-to-noise ratio. The pre-processing steps for images taken from sources other than the 1-m ST were also performed in a similar fashion.

Fig. 1 shows the location of SN 2008gz in the galaxy NGC 3672. The SN flux is expected to have a substantial contribution from the host-galaxy background, due to its proximity to the galaxy centre, its location in a spiral arm and the high inclination angle (56.°2; Table 1) of the galaxy. At early phases the SN flux dominates the total flux, thus with a PSF-fitting method we were able to remove the galaxy contribution. At later epochs (e.g. the end of the plateau in the case of Type IIP events), the galaxy flux may brighten the SN light curves by 0.5–1 mag depending on its location in the galaxy (Pastorello et al. 2005). We used ISIS[5] (Alard & Lupton 1998) to obtain the galaxy-template-subtracted flux of the supernova. As a template we used the *BVRI* images taken on 2010 February 14 (+548 d) from the 1-m ST, India in good seeing conditions. We note that the galaxy subtraction using pre-SN (−403 d) *VRI* images taken from Perth Observatory gave no SN contribution above the noise level in our images recorded on 2009 November 19 and 2010 February 13 and 14. In order to verify the ISIS results, we also performed the galaxy-template-subtraction scheme independently using self-written scripts employing IRAF tasks which included alignment, PSF and intensity matching of the galaxy template and SN images and

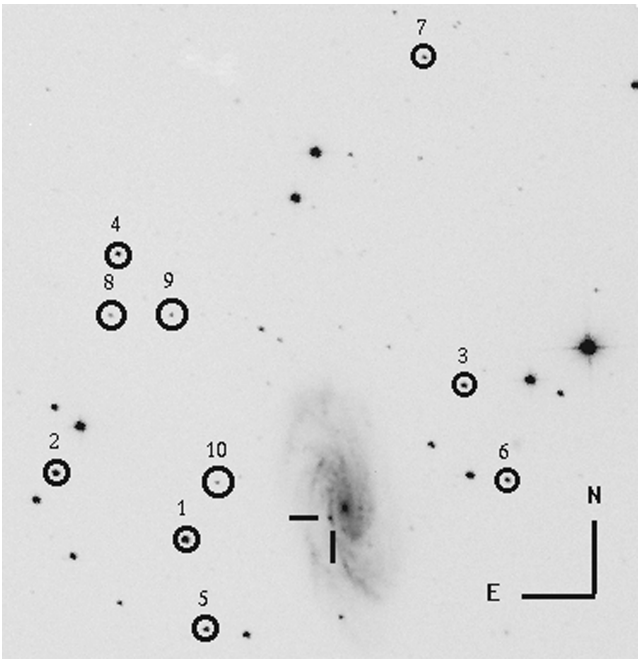


**Figure 1.** SN 2008gz in NGC 3672. *V*-band image from the 1-m ST, India. An area of about 8 × 8 arcmin$^2$ is shown, with the location of the SN marked with a cross and reference standard stars marked with circles.

subtraction of the template from the SN images. Fig. 2 shows images with and without template subtraction. The PSF-fitting method was applied to the subtracted images. Our magnitudes were found to be consistent with the ISIS ones, having a typical scatter of ∼0.1 mag in *BVRI*; this scatter is of the order of 0.05 mag in the plateau phase (see Fig. 3).[6]

In order to calibrate the instrumental magnitudes of SN 2008gz, we observed Landolt (2009) standard fields SA92 and PG0231 in *BVRI* with the 1-m ST on 2008 November 15 under good night conditions (transparent sky, FWHM seeing with $V \sim 2$ arcsec). The data reduction of SN and Landolt fields was done using a profile-fitting technique and the instrumental magnitudes were converted into the standard system following the least-squares linear regression procedures outlined in Stetson (1992). We used mean values of atmospheric extinction coefficients of the site, namely 0.28, 0.17, 0.11 and 0.07 mag per unit airmass for the $B, V, R$ and $I$ bands respectively (Kumar et al. 2000). A set of 13 stars having a colour range of $-0.33 \leq (B - V) \leq 1.45$ and brightness range of $12.77 \leq V \leq 16.11$ was used to derive the following zero-points and colour

[2] The full version of Table 2 is available only in electronic form – see Supporting Information.

[3] IRAF stands for Image Reduction and Analysis Facility distributed by the National Optical Astronomy Observatories which is operated by the Association of Universities for research in Astronomy, Inc. under co-operative agreement with the National Science Foundation.

[4] DAOPHOT stands for Dominion Astrophysical Observatory Photometry.

[5] http://www2.iap.fr/users/alard/package.html

[6] Fig. 3 is available only in electronic form – see Supporting Information.

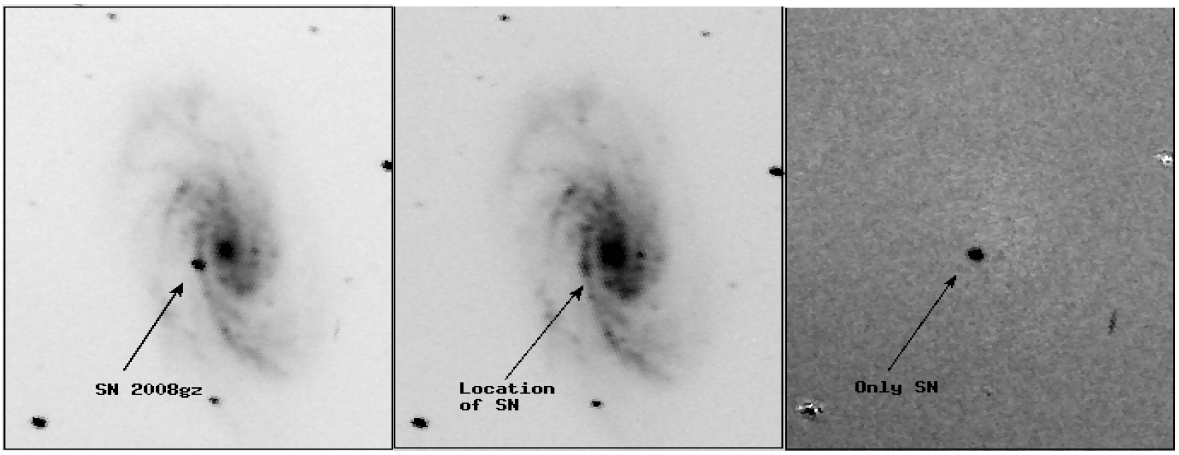


**Figure 2.** Template subtraction for SN 2008gz. The $V$-band image from 2008 December 10 (+117 d) with the SN is shown in the leftmost panel, the template frame from 2010 February 14 (+548 d) without the SN in the middle and the template-subtracted image in the rightmost panel. All the images are around 3 × 4.5 arcmin$^2$. North is up and east is to the left.

**Table 3.** Identification number (ID), coordinates ($\alpha$, $\delta$) and calibrated magnitudes of stable secondary standard stars in the field of SN 2008gz. Errors in magnitude represent RMS scatter in the night-to-night repeatability over the entire period of SN monitoring.

| Star ID | $\alpha_{J2000}$ (h m s) | $\delta_{J2000}$ ($^\circ$ $'$ $''$) | $B$ (mag) | $V$ (mag) | $R$ (mag) | $I$ (mag) |
|---|---|---|---|---|---|---|
| 1 | 11 25 11.27 | −09 48 04.4 | 15.36 ± 0.01 | 14.36 ± 0.03 | 13.99 ± 0.01 | 13.49 ± 0.01 |
| 2 | 11 25 18.34 | −09 47 03.0 | 15.70 ± 0.01 | 14.92 ± 0.02 | 14.68 ± 0.01 | 14.25 ± 0.01 |
| 3 | 11 24 55.62 | −09 46 07.9 | 16.50 ± 0.01 | 15.82 ± 0.03 | 15.64 ± 0.01 | 15.26 ± 0.01 |
| 4 | 11 25 14.22 | −09 44 04.7 | 16.91 ± 0.01 | 16.15 ± 0.01 | 15.93 ± 0.01 | 15.50 ± 0.01 |
| 5 | 11 25 10.47 | −09 49 17.0 | 17.00 ± 0.02 | 16.23 ± 0.03 | 15.98 ± 0.01 | 15.52 ± 0.04 |
| 6 | 11 24 53.17 | −09 47 25.1 | 17.09 ± 0.02 | 16.42 ± 0.03 | 16.22 ± 0.01 | 15.83 ± 0.03 |
| 7 | 11 24 56.67 | −09 41 35.1 | 17.80 ± 0.02 | 16.99 ± 0.02 | 16.66 ± 0.01 | 16.19 ± 0.04 |
| 8 | 11 25 14.78 | −09 44 54.3 | 18.50 ± 0.07 | 17.70 ± 0.07 | 17.49 ± 0.06 | 17.12 ± 0.03 |
| 9 | 11 25 11.40 | −09 44 54.5 | 18.28 ± 0.04 | 17.75 ± 0.03 | 17.62 ± 0.02 | 17.22 ± 0.04 |
| 10 | 11 25 09.31 | −09 47 16.4 | 18.83 ± 0.09 | 17.92 ± 0.07 | 17.63 ± 0.03 | 17.08 ± 0.06 |

coefficients:

$$b = B + (5.37 \pm 0.02) + (0.01 \pm 0.02)(B - V),$$

$$v = V + (4.89 \pm 0.01) + (-0.02 \pm 0.02)(B - V),$$

$$r = R + (4.72 \pm 0.01) + (0.02 \pm 0.02)(V - R),$$

$$i = I + (5.17 \pm 0.02) + (0.02 \pm 0.02)(V - I).$$

Here $B, V, R, I$ are the standard magnitudes and $B, V, R, I$ are corresponding instrumental magnitudes corrected for time and aperture. A typical scatter in the photometric solutions to the Landolt standard stars is found to be ∼0.03 mag for *BVRI*. Table 3 lists the calibrated magnitudes for a set of ten stable secondary standards in the SN field, while calibrated *BVRI* magnitudes of SN 2008gz are presented in Table 4. For SN, we quote ISIS-derived errors ($1\sigma$ uncertainty), which is consistent with the root-mean square (RMS) scatter in the magnitude of standard stars determined from night-to-night repeatability over the entire period (∼215 d) of SN monitoring. Large errors in the 2-m IGO and 3.6-m NTT data arise due to a mismatch in the PSF and pixel scale.

### 2.2 Optical light curve

Fig. 4 shows *BVRI* light curves of SN 2008gz ranging from +87 d to +275 d since the time of explosion. We also present the light curves of other well-studied nearby ($D < 12$ Mpc) Type IIP SNe, namely 2004et (Sahu et al. 2006; Misra et al. 2007), 1999em (Elmhamdi et al. 2003a) and 1999gi (Leonard, Filippenko & Gates 2002), scaled in time and magnitude to match the transition between plateau and nebular phases. It is seen that SN 2008gz was detected close to the end of its plateau phase and its light curve strongly resembles the above three template IIP events; hence we could determine (and adopt) a time of inflection (plateau to nebular) $t_i$ of 115 ± 5 d by adjusting the template light curves to obtain the best match to SN 2008gz data points. This derived plateau duration is typical for Type IIP events (Elmhamdi, Chugai & Danziger 2003b) and is also consistent with the fact that SN 2008gz was not visible around three months before the discovery date (2008 November 5.83) at a level of unfiltered magnitude of 19.0 (Nakano & Martin 2008). Further, similarities between the bolometric tail luminosity of SN 2008gz (see Section 7) and those of SN 2004et and SN 1999em indicate that probably the explosion happened about 82 d before the discovery date. Analysis of the first spectrum of SN 2008gz (see Section 3.2) also revealed a few similarities between the kinematical properties of its ejecta and those of SN 2004et observed nearly 80 d after the burst. We therefore adopt the time of SN explosion as 82 ± 5 d before the discovery date and this corresponds to a burst time $t_0$ of JD 245 4694.0; however, we note that based on the first spectrum (2008 November 11.25 UT) and its similarity to the +62 d spectrum of SN 1998A (Benetti et al. 2008), the suggestion of a time of explosion of nearly 56 d before the discovery date (corresponding to a plateau phase of ∼90 d) cannot be ruled out.

**Table 4.** Photometric evolution of SN 2008gz. Errors in magnitude are derived from ISIS and denote $1\sigma$ uncertainty.

| UT Date (yy/mm/dd) | JD 245 4000+ | Phase[a] (day) | $B$ (mag) | $V$ (mag) | $R$ (mag) | $I$ (mag) | Telescope[b] | Seeing[c] ($''$) |
|---|---|---|---|---|---|---|---|---|
| 2008/11/10 | 781.47 | +87 | 17.205 ± 0.016 | 15.871 ± 0.012 | 15.475 ± 0.008 | 15.168 ± 0.015 | ST | 2.4 |
| 2008/11/11 | 782.49 | +88 | 17.312 ± 0.030 | 15.819 ± 0.014 | 15.477 ± 0.010 | 15.164 ± 0.013 | ST | 2.6 |
| 2008/11/15 | 786.47 | +92 | 17.355 ± 0.040 | 15.918 ± 0.019 | 15.501 ± 0.013 | 15.189 ± 0.017 | ST | 2.7 |
| 2008/11/16 | 787.47 | +93 | 17.376 ± 0.033 | 15.920 ± 0.017 | 15.537 ± 0.011 | 15.210 ± 0.014 | ST | 2.4 |
| 2008/11/17 | 788.48 | +94 | 17.402 ± 0.030 | 15.957 ± 0.017 | 15.552 ± 0.011 | 15.207 ± 0.016 | ST | 2.4 |
| 2008/11/18 | 789.46 | +95 | 17.457 ± 0.037 | 15.966 ± 0.021 | 15.533 ± 0.012 | 15.219 ± 0.015 | ST | 3.3 |
| 2008/11/23 | 794.47 | +100 | 17.550 ± 0.033 | 16.002 ± 0.020 | 15.587 ± 0.015 | 15.373 ± 0.019 | ST | 3.5 |
| 2008/11/26 | 797.47 | +103 | 17.684 ± 0.014 | 16.182 ± 0.008 | 15.685 ± 0.003 | 15.373 ± 0.005 | ST | 2.7 |
| 2008/11/28 | 799.45 | +105 | 17.703 ± 0.029 | 16.228 ± 0.018 | 15.732 ± 0.014 | 15.397 ± 0.021 | ST | 3.0 |
| 2008/12/01 | 802.49 | +108 | 17.900 ± 0.028 | 16.311 ± 0.017 | 15.830 ± 0.011 | 15.475 ± 0.017 | ST | 2.5 |
| 2008/12/10 | 811.49 | +117 | 18.342 ± 0.037 | 16.702 ± 0.027 | 16.151 ± 0.017 | 15.761 ± 0.026 | ST | 2.9 |
| 2008/12/21 | 822.49 | +128 | 19.125 ± 0.094 | 17.519 ± 0.047 | 16.857 ± 0.026 | 16.480 ± 0.040 | ST | 2.6 |
| 2008/12/22 | 823.46 | +129 | 19.190 ± 0.073 | 17.597 ± 0.043 | 16.909 ± 0.023 | 16.583 ± 0.029 | ST | 2.3 |
| 2008/12/24 | 825.53 | +131 | 19.242 ± 0.174 | 17.695 ± 0.058 | 16.893 ± 0.022 | 16.393 ± 0.026 | ST | 3.6 |
| 2008/12/26 | 827.52 | +133 | 19.044 ± 0.176 | 17.638 ± 0.036 | 16.982 ± 0.017 | 16.546 ± 0.024 | ST | 3.1 |
| 2008/12/28 | 829.44 | +135 | – | 17.704 ± 0.037 | 16.928 ± 0.020 | 16.559 ± 0.026 | ST | 2.7 |
| 2008/12/29 | 830.49 | +136 | 19.165 ± 0.085 | 17.674 ± 0.039 | 16.976 ± 0.021 | 16.582 ± 0.041 | ST | 3.2 |
| 2009/01/01 | 833.52 | +139 | – | 17.738 ± 0.047 | 17.016 ± 0.021 | 16.623 ± 0.030 | ST | 2.7 |
| 2009/01/08 | 840.48 | +146 | 19.547 ± 0.121 | 17.684 ± 0.043 | 17.069 ± 0.024 | 16.671 ± 0.049 | ST | 3.1 |
| 2009/01/18 | 850.36 | +156 | 19.489 ± 0.168 | 17.920 ± 0.082 | 17.118 ± 0.040 | 16.717 ± 0.055 | ST | 3.1 |
| 2009/01/19 | 851.32 | +157 | 19.631 ± 0.156 | 17.941 ± 0.068 | 17.128 ± 0.033 | 16.779 ± 0.061 | ST | 3.1 |
| 2009/01/21 | 853.48 | +159 | 19.115 ± 0.069 | 18.027 ± 0.078 | 17.128 ± 0.038 | 16.688 ± 0.049 | ST | 3.2 |
| 2009/01/23 | 855.51 | +161 | 19.373 ± 0.077 | 18.000 ± 0.102 | 17.178 ± 0.036 | – | ST | 3.1 |
| 2009/01/27 | 859.36 | +165 | 19.699 ± 0.096 | 18.002 ± 0.054 | 17.279 ± 0.029 | 16.877 ± 0.045 | ST | 2.2 |
| 2009/02/01 | 864.35 | +170 | 19.498 ± 0.093 | 18.019 ± 0.062 | 17.305 ± 0.032 | 16.903 ± 0.047 | ST | 2.5 |
| 2009/02/16 | 879.42 | +185 | 19.461 ± 0.096 | 18.217 ± 0.065 | 17.434 ± 0.032 | 17.029 ± 0.046 | ST | 2.4 |
| 2009/02/17 | 880.27 | +186 | 19.684 ± 0.095 | 18.181 ± 0.064 | 17.420 ± 0.030 | 17.087 ± 0.046 | ST | 2.9 |
| 2009/02/20 | 883.34 | +189 | 19.609 ± 0.124 | 18.179 ± 0.075 | 17.434 ± 0.039 | 17.071 ± 0.058 | ST | 3.2 |
| 2009/02/26 | 889.27 | +195 | 19.467 ± 0.113 | 18.269 ± 0.093 | 17.468 ± 0.045 | 17.121 ± 0.068 | ST | 3.6 |
| 2009/03/04 | 895.23 | +201 | 18.976 ± 0.118 | 18.163 ± 0.111 | 17.417 ± 0.052 | 16.924 ± 0.070 | ST | 3.0[d] |
| 2009/03/21 | 912.33 | +218 | 19.665 ± 0.877 | 18.380 ± 0.341 | 17.720 ± 0.125 | 17.373 ± 0.181 | IGO | 1.6 |
| 2009/03/22 | 913.24 | +219 | 19.681 ± 0.775 | 18.441 ± 0.335 | 17.762 ± 0.128 | 17.366 ± 0.196 | IGO | 1.6 |
| 2009/03/24 | 915.32 | +221 | 19.552 ± 0.712 | 18.601 ± 0.292 | 17.714 ± 0.104 | 17.449 ± 0.165 | IGO | 1.5 |
| 2009/03/25 | 916.30 | +222 | 19.545 ± 0.727 | 18.416 ± 0.320 | 17.723 ± 0.117 | 17.362 ± 0.171 | IGO | 1.4 |
| 2009/03/26 | 917.32 | +223 | 20.029 ± 0.188 | 18.743 ± 0.143 | 17.710 ± 0.057 | 17.463 ± 0.107 | ST | 3.5 |
| 2009/04/03 | 925.20 | +231 | 19.414 ± 0.372 | 18.701 ± 0.242 | 17.899 ± 0.083 | 17.481 ± 0.130 | ST | 2.8 |
| 2009/04/12 | 934.29 | +240 | – | 18.807 ± 0.257 | 17.888 ± 0.089 | 17.680 ± 0.124 | ST | 2.7 |
| 2009/04/17 | 939.23 | +245 | 21.040 ± 0.270 | 18.909 ± 0.132 | 18.000 ± 0.052 | 17.680 ± 0.080 | ST | 2.8 |
| 2009/04/23 | 945.16 | +251 | 19.878 ± 0.187 | 19.005 ± 0.165 | 18.176 ± 0.093 | 17.730 ± 0.145 | ST | 3.1 |
| 2009/05/01 | 953.15 | +259 | 19.633 ± 0.182 | 18.760 ± 0.199 | 18.254 ± 0.080 | 17.822 ± 0.109 | ST | 2.5 |
| 2009/05/17 | 969.11 | +275 | 20.388 ± 0.984 | 19.173 ± 0.556 | 18.383 ± 0.269 | 18.099 ± 0.281 | NTT | 0.9 |

[a]With reference to the explosion epoch JD 245 4694.0.
[b]ST: 1-m Sampurnanand Telescope, ARIES, India; IGO: 2-m IUCAA Girawali Observatory, IUCAA, India; NTT: 3.6-m New Technology Telescope, ESO, Chile.
[c]FWHM of the stellar PSF in the $V$ band.
[d]Flat-field problem.

In the late plateau phase ($\sim +90$ d), the flatness behaviour in $RI$ and decline trend in $BV$ are clearly seen, similarly to other IIP events. The $V$ magnitude drop of 1.5 mag from the plateau phase ($V \sim 16$ mag at +100 d) to the nebular phase (17.5 mag at +130 d) is slightly lower than the 2–3 mag drop for a typical IIP event (Olivares et al. 2010). This shallow decline is seen in $BRI$ also, indicating the production of a large $^{56}$Ni mass (see Section 8.1). In contrast to this, a very steep brightness decline in $V$ has also been observed, e.g. 4.5 mag for SN 2007od (Andrews et al. 2010). The nebular phase starts at $\sim +140$ d and roughly follows the decay slope of $^{56}$Co to $^{56}$Fe : 0.98 mag (100 d)$^{-1}$. A linear fit to the tail from +150 d to +275 d gives the following decline rates [in mag (100 d)$^{-1}$]: $\gamma_B \sim 0.51, \gamma_V \sim 0.98, \gamma_R \sim 1.12, \gamma_I \sim 1.13$ in $B, V, R, I$, which is typical of the values found for IIP SNe. The flattening seen in the $B$-band light curve, though non-conclusive due to the large scatter of the measurements, has also been observed in other events, e.g. in 1999em (Elmhamdi et al. 2003a) and 1987A (Suntzeff et al. 1988) until +400 d.

## 3 LOW-RESOLUTION SPECTROSCOPY

### 3.1 Data

Long-slit low-resolution spectra (∼6–14 Å) in the optical range (0.33–1.0 μm) were collected at eight epochs between +87 and +275 d: five epochs from the 2-m IGO and one epoch each from the 3.5-m TNG, 6-m BTA and 3.6-m NTT. The journal of spectroscopic observations is given in Table 5.

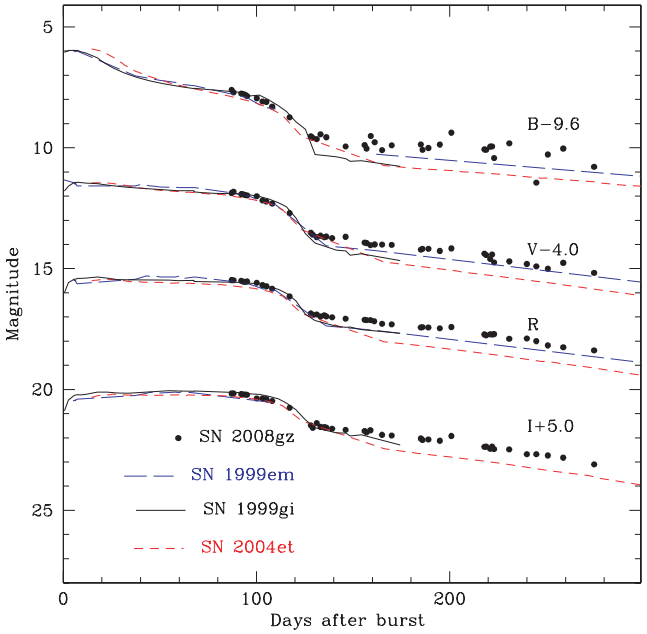


**Figure 4.** Light curve in *BVRI* magnitudes of SN 2008gz. The light curves are shifted for clarity, while for other SNe they are scaled in magnitude and time to match with SN 2008gz.

At the 2-m IGO, observations were carried out using IFOSC mounted at the Cassegrain end of a $f/10$ reflector (Gupta et al. 2002; Chakraborty, Das & Tandon 2005). Slit spectra were recorded using a 2048 × 2048 EEV CCD camera with 13.5-μm pixels, having a gain of 1.8 $e^-$ per analogue-to-digital unit and a readout noise of 6.3 $e^-$. Grism 7 with peak sensitivity at 500 nm and a slit width of 1.5 arcsec were used. Calibration frames (bias, flats, arcs) and spectrophotometric flux standards were observed on each night. For SN, usually slits were placed across the spiral arm so as to make a proper sky background, and in one case at +170 d the galaxy centre was also observed. Spectroscopic data reduction was done under the IRAF environment. Bias and flat-fielding were performed on each frame. Cosmic-ray rejection on each frame was carried out using Laplacian kernel detection (van Dokkum 2001). Images were co-added to improve the signal-to-noise ratio and one-dimensional spectra were extracted using the apall task in IRAF, which is based on the optimal-extraction algorithm by Horne (1986). Wavelength calibration was performed using the identify task and about 15–18 emission lines of He and Ar, which were used to find a dispersion solution. Fifth-order fits were used to achieve a typical RMS uncertainty of 0.1 Å. The position of the O I emission skyline at 5577 Å was used to check the wavelength calibration, and deviations were found between 0.5 and 1 Å; this was corrected by a linear shift in dispersion. The instrumental FWHM resolution of the 2-m IGO spectra as measured from the O I 5577-Å emission skyline was found to lie in range 6–10 Å (∼322–510 km $s^{-1}$). Flux calibration was done using spectrophotometric fluxes from Hamuy et al. (1994) and assuming a mean extinction for the site. Synthetic magnitudes were estimated using spectra to verify the accuracy of flux calibration and were found to be accurate to within 0.05 mag.

Spectroscopic data reduction for DOLORES on the 3.6-m TNG, EFOSC2 on the 3.6-m NTT and SCORPIO on the 6-m BTA was carried out in a similar fashion, and at around 6000 Å had a resolution of 10, 14 and 12 Å, respectively.

### 3.2 Optical spectra

Figs 5 and 6 show the rest-frame spectra of SN 2008gz, corrected for the recession velocity (1864 km $s^{-1}$) of the host galaxy NGC 3672. We identify all the spectral features as per previously published line identifications for IIP events (Leonard et al. 2002; Sahu et al. 2006). In Fig. 5, the end of the plateau phase (+115 d) and beginning of the nebular phase (+140 d) are clearly evident in the spectral evolution.

The late plateau-phase (+87 d and +115 d) spectra are marked by strong P Cygni features of H$\alpha$, O I 7700 Å, Na I D 5890, 5896 Å and singly ionized Sc, Ba, Ti, Fe atoms, while the +140 d and later spectra show a significant drop in the absorption strength of P Cygni features. The spectra during +115 d to +222 d show the spectral evolution of the event from the early to mid-nebular stage, while the last two spectra (+231 d and +275 d) are those typically seen during the late stages of a typical SNIIP. In Fig. 6, the +87 d spectrum shows various atomic absorption lines over a weak continuum. These lines are mainly due to elements present in the SN ejecta along with some earth atmospheric molecular lines (marked with ⊕) and absorption due to Na I D in the Milky Way and host galaxy. On the other hand, the +275 d spectrum shows a typical nebular-phase spectrum dominated by emission lines.

**Table 5.** Journal of spectroscopic observations of SN 2008gz.

| UT Date (yy/mm/dd/hh.hh) | JD 245 4000+ | Phase[a] (days) | Range (μm) | Telescope[b] | Grating (gr $mm^{-1}$) | Slit width (″) | Dispersion (Å $pix^{-1}$) | Exposure (s) | S/N[c] ($pix^{-1}$) |
|---|---|---|---|---|---|---|---|---|---|
| 2008/11/11/06.049 | 781.88 | +87 | 0.34−0.80 | TNG | 500 | 1.5 | 2.5 | 1200 | 80 |
| 2008/12/08/23.346 | 809.46 | +115 | 0.38−0.68 | IGO | 600 | 1.5 | 1.4 | 2x1800 | 50 |
| 2009/01/03/00.333 | 834.52 | +140 | 0.38−0.68 | IGO | 600 | 1.5 | 1.4 | 2x1800 | 26 |
| 2009/02/01/22.208[d] | 864.40 | +170 | 0.38−0.68 | IGO | 600 | 1.5 | 1.4 | 2x1800 | 20 |
| 2009/02/02/21.400 | 865.40 | +171 | 0.38−0.68 | IGO | 600 | 1.5 | 1.4 | 3x1800 | 24 |
| 2009/03/22/18.303 | 913.27 | +218 | 0.38−0.68 | IGO | 600 | 1.5 | 1.4 | 1800 | 8 |
| 2009/03/25/19.673 | 916.33 | +222 | 0.38−0.68 | IGO | 600 | 1.5 | 1.4 | 1800 | 7 |
| 2009/04/03/22.643 | 924.50 | +231 | 0.61−1.00 | BTA | 550 | 2.1 | 3.5 | 3x900 | 70 |
| 2009/05/17/00.543 | 969.04 | +275 | 0.33−0.80 | NTT | 300 | 1.0 | 4.0 | 2700 | 16 |
| 2009/05/17/01.308 | 969.07 | +275 | 0.55−1.05 | NTT | 300 | 1.0 | 4.2 | 2700 | 24 |

[a]With reference to the burst time JD 245 4694.0.
[b]TNG: DOLORES on 3.5-m Telescopio Nazionale Galileo, Canary Islands; IGO: IFOSC on 2-m IUCAA Girawali Observatory, India; BTA: SCORPIO on 6-m Big Telescope Alt-azimuthal, Special Astrophysical Observatory, Russia; NTT: EFOSC2 on 3.6-m New Technology Telescope, ESO, Chile.
[c]At 0.6 μm.
[d]Only centre of galaxy observed.

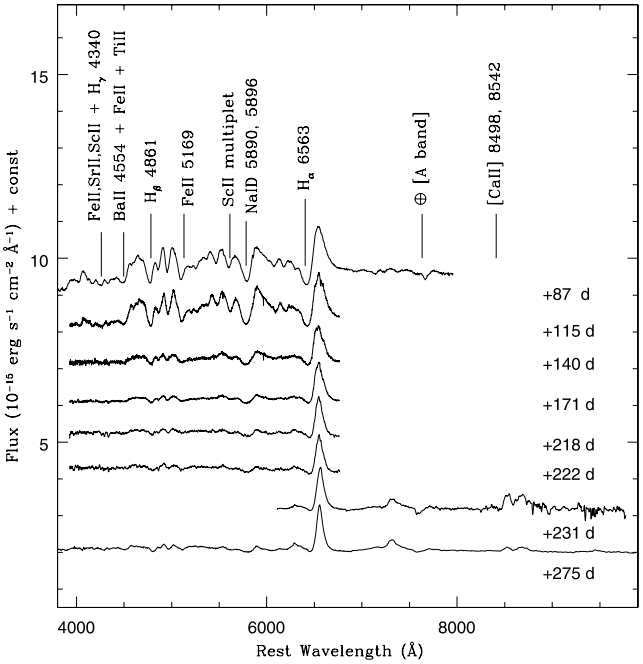


**Figure 5.** Doppler-corrected flux spectra of SN 2008gz from the late plateau (+87 d) to the nebular phase (+275 d). Prominent hydrogen and metal lines are marked.

Temporal evolution of the P Cygni nature of H$\alpha$ is clearly seen; namely the emission component becomes narrower, with a decrease in depth of the associated absorption component, during the transition of the SN from plateau to nebular phases. The FWHM of the emission component of H$\alpha$ decreases from $\sim$5477 km s$^{-1}$ at +87 d to $\sim$3526 km s$^{-1}$ at +275d, indicating a decrease in opacity and temperature of the H I line-emitting regions. For H$\beta$, H$\gamma$ and H$\delta$, the emission components are crowded with numerous metal lines. In Fig. 6, we also see the impression of an additional P Cygni component in the absorption profile of H$\alpha$ and H$\beta$. This is speculated as a footprint of high-velocity emitting shells in the SN ejecta. Similar signatures were also noticed in the Type IIP SNe 1999em and 2004et (Leonard et al. 2002; Li et al. 2005; Sahu et al. 2006).

The spectrum, labelled with +275 d, shows a typical late nebular-phase spectrum marked by emission-dominated permitted lines of Ca II 8498, 8542, 8662 Å and Na I D as well as the appearance of forbidden emission lines, i.e. [O I] 6300, 6364 Å; [Fe II] 7155 Å and [Ca II] 7291, 7324 Å. These forbidden lines are not observed on Earth due to the high density of gas. [Ca II] is already seen in the +87 d spectrum and [O I] appears at +171 d, while [Fe II] appears in the +275 d spectrum. The increasing strength of these forbidden lines indicates the expansion and rarefaction of SN ejecta with time. The [Fe II] line was also noticed by Pastorello et al. (2005) in the +344 d spectrum of SN 1998A and +346 d spectrum of SN 1987A, whereas for low-luminosity SN 1997D it was visible at +417 d (Benetti et al. 2001). We determine a relative strength $I$([Ca II])/$I$([Fe II]) of 2.06 for SN 2008gz, whereas for SNe 1999em and 1987A values of this ratio are respectively 6.98 and 24.68 at around +400 d (Elmhamdi et al. 2003a). This indicates that the physical conditions of [Fe II] formation in SN 2008gz may be similar to those in SN 1999em rather than SN 1987A.

## 4 TEMPORAL EVOLUTION OF SPECTRAL LINES

To illustrate further the nature of the burst, we show in Fig. 7 (and describe below) the velocity profiles of H$\alpha$, H$\beta$, Na I D, Ba II 6142 Å and [O I]6300, 6364 Å. The absorption dips and emission peaks due to the SN are marked by downward and upward arrows respectively. For a spherically symmetric burst, the emission peak of P Cygni profiles should be located at the rest wavelength of the corresponding line, while the absorption dip will be blueshifted, reflecting the instantaneous velocity of the corresponding line-emitting region. In our rest-frame spectra, the H$\alpha$ emission peak is found to be slightly blueshifted by $\sim$406 km s$^{-1}$ at +87 d. Such a blueshift in the H$\alpha$ emission peak at early epochs was also observed for other Type II SNe (1987A – Hanuschik & Dachs 1987; 1988A – Turatto et al. 1993; 1990K – Cappellaro et al. 1995; 1993J – Matheson et al. 2000; 1998A – Pastorello et al. 2005; 1999em – Elmhamdi et al. 2003a; 2005cs – Pastorello et al. 2009; 2007od – Andrews et al. 2010). It is observed for a few low-luminosity Type II SNe as well, e.g. SN 1999br in the early phases (Pastorello et al. 2004). On the basis of the SN 1987A velocity profile, Chugai (1988) explained this phenomenon as an effect of the diffused reflection of resonance radiation by the expanding photosphere. For SN 1987A at +85 d this velocity was about a few hundred km s$^{-1}$ and hence comparable with SN 2008gz. On the other hand, for SN 1998A and SN 1993J the H$\alpha$ emission-peak velocity at a comparable epoch was at least one order of magnitude higher than for SN 2008gz. At a later epoch (+275 d), the H$\alpha$ emission-peak velocity for SN 2008gz is about $-$200 km s$^{-1}$, which is considerably different from SN 1987A where a redshifted velocity of +600 km s$^{-1}$ was observed.

In most of our H$\alpha$ profiles, a narrow emission line (marked by 'D' in Fig. 7) is seen at zero velocity, which is probably due to the underlying H II region; this is consistent with the presence of a low-luminosity H II region at the SN location revealed by our H$\alpha$ narrow-band observation (Section 8.2). Such a feature is not seen in the well-observed nearby IIP SNe 2004et (Sahu et al. 2006) and 2004A (Gurugubelli et al. 2008), which occurred on the outskirts of their host galaxies.

The P Cygni nature of Na I D 5892 Å is prominent in the spectra at all epochs with an emission peak located at zero velocity, indicating an almost spherical distribution of the Na ion in the ejected material. In the high S/N spectra (+87 d and +115 d), two peculiar absorption dips in the SN Na I D emission profile are seen at $-$80 km s$^{-1}$ (marked by B) and $-$1630 km s$^{-1}$ (marked by C), respectively. These are identified as Na I D absorption due to interstellar matter in the host galaxy and the Milky Way respectively (Section 6). In this regard we note that, due to a highly inclined host galaxy ($\Theta_{\rm inc} = 56.^{\circ}2$), the true recession velocity for the SN will be different from the adopted one (1864 km s$^{-1}$), and as measured from Na I D absorption at the SN location it should differ by $\sim$100 km s$^{-1}$; however, considering low-dispersion spectra, this will not change any of our conclusions.

The absorption dips due to s-process element Ba II 6142 Å and the element Sc II 6248 Å are clearly visible in the +87 d and +115 d spectra, however they have disappeared in the +140 d spectrum. This is similar to the luminous Type IIP SNe 2004et (Sahu et al. 2006), where these lines were prominent at +113 d and barely observable at +163 d, and 1999em (Elmhamdi et al. 2003a), where they were visible up to +166 d. In contrast to this, in low-luminosity IIP SNe 1997D, 2005cs and others (Turatto et al. 1998; Benetti et al. 2001; Pastorello et al. 2004) these features are sustained for a comparatively longer time and observable till +208 d. Low-luminosity

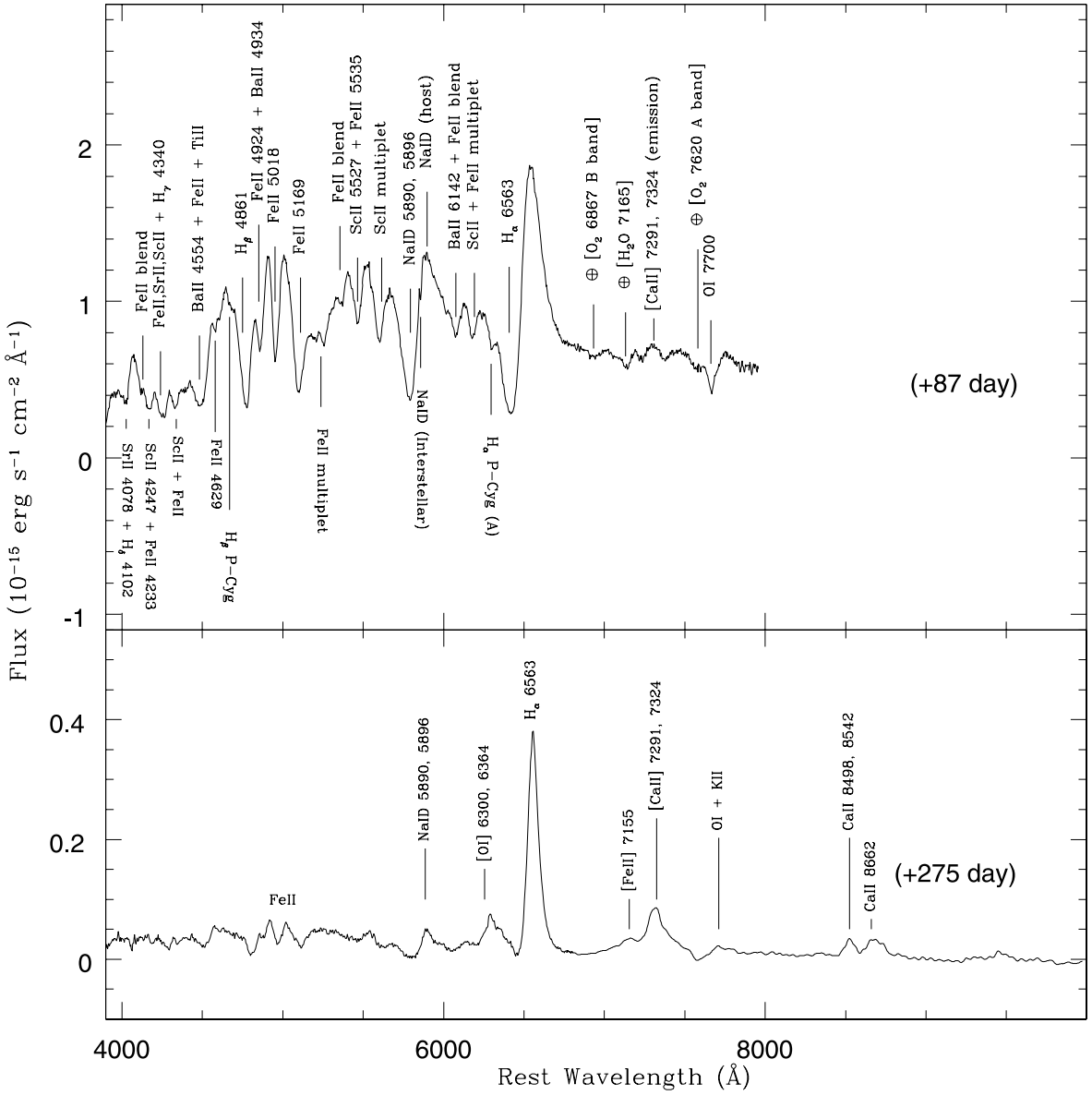


**Figure 6.** Line identification for the late plateau and deep nebular phases.

Type IIP SNe expand with a velocity much slower than that of normal Type IIP events, so the Ba lines in low-luminosity events are sustained for a longer time just because the ejecta takes more time to cool down. For luminous Type II peculiar SNe 1987A and 1998A, these feature are seen even at later epochs beyond +300 d. For SN 2008gz, probably the Ba abundance was low and the s-process not so effective as in low-luminosity events.

Metastable [O I] 6300, 6364 Å lines start to appear at +171 d, and their strength increases progressively in spectra at later epochs. A normalized profile for +275 d is shown in Fig. 8,[7] which is nearly symmetric, indicating spherically symmetric oxygen ejecta. The average FWHM for [O I] lines is $\sim$2500 km s$^{-1}$. A two-component Gaussian fit results in a ratio of $I(6300)/I(6364) \approx 1.8$, which deviates from the strength ratio of 3 expected from the transitional probability for a rarefied gas at a certain temperature. The smaller ratio for SN 2008gz may indicate higher opacity for 6300 Å in comparison with 6364 Å. We note, however, that the ratio of $I(6300)/I(6364)$ is not always 3 for Type IIP events. For SN 1988A, Spyromilio (1991) showed that at initial epochs when the optical depth of the ejecta is very high, the value of $I(6300)/I(6364)$ is $\approx$0.952, whereas in the late phase for optically thin ejecta this ratio approaches 3.03.

The blueshift in [O I] lines, particularly at epochs later than +400 d (i.e. in SNe 1999em and 1987A), is interpreted as an effective indicator of dust formation in SN ejecta due to excessive extinction of the redshifted wings of emission lines compared with the blueshifted ones (Lucy et al. 1991; Danziger et al. 1991). Between +300 and 400 d, the observed blueshift in oxygen may be due to contamination from the Fe II mutliplet at 6250 AA. The reason for the blueshift of the oxygen line at early epochs ($\lesssim$200 d) is still not clear and several hypothesis have been suggested. In a recent work, Taubenberger et al. (2009) described this as a result of residual opacity that remains in the inner ejecta. This seems to be the most likely explanation for the observed blueshift of the oxygen line. Dust formation at an early epoch $\sim$ +300 d is also reported for

[7] Fig. 8 is available only in electronic form – see Supporting Information.

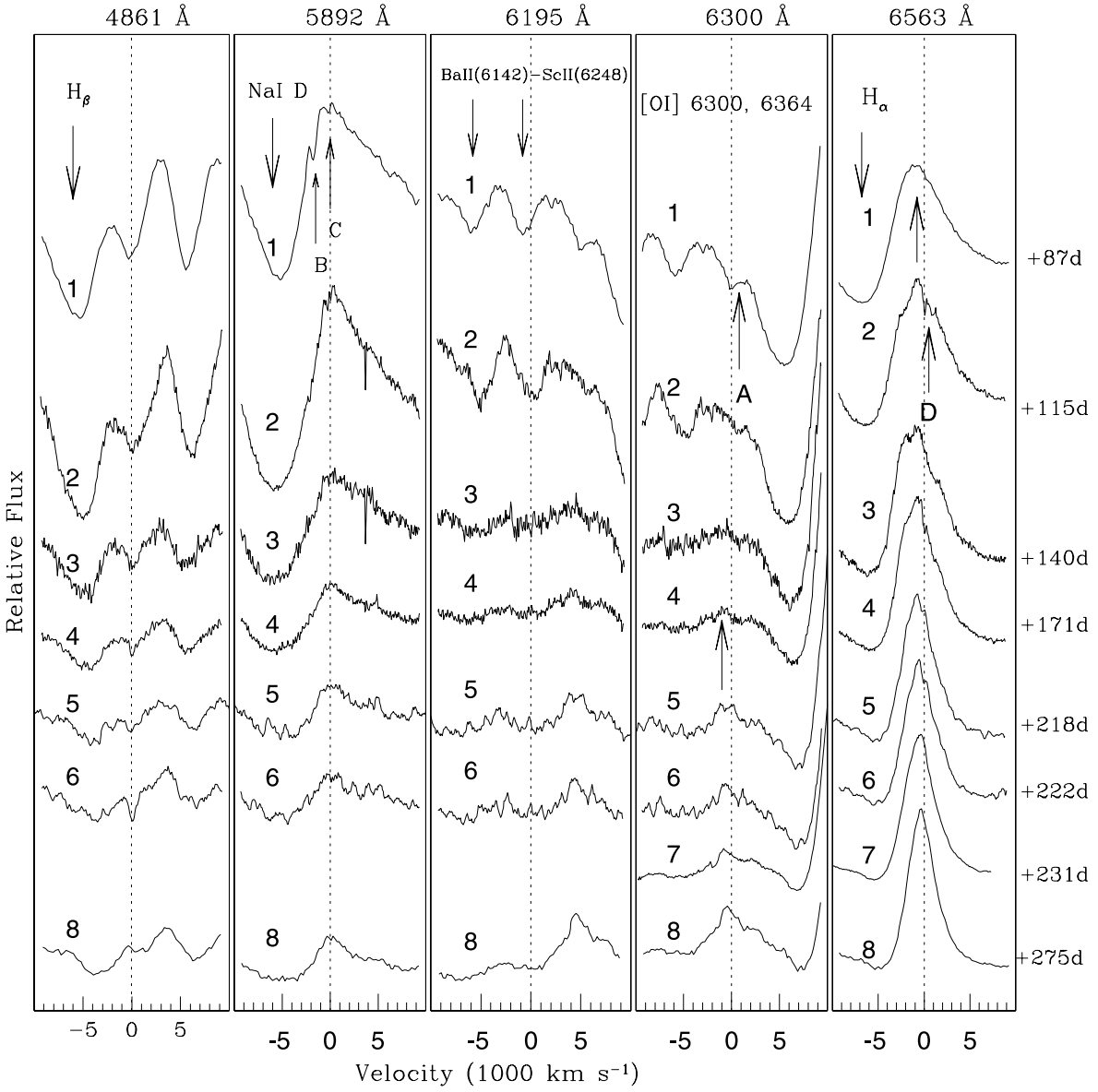


**Figure 7.** Evolution of some important spectral lines of SN 2008gz during its transition from late plateau to nebular phases. The dotted line at zero velocity corresponds to the rest wavelength. Upward arrows show emission peaks, while downward arrows show absorption dips. The feature 'A' is a high-velocity P Cygni component of H$\alpha$, features 'B' and 'C' are due to Na I D absorption from the Milky Way and the host respectively, and the emission feature 'D' is H$\alpha$ emission due to the underlying H II region at the SN location. The numbering sequences and resolution are (1) +87 d/10 Å, (2) +115 d/6 Å, (3) +140 d/12 Å, (4) +171 d/6 Å, (5) +218 d/10 Å, (6) +222 d/10 Å, (7) +231 d/10 Å and (8) +275 d/14 Å.

SN 2004et. For SN 2008gz we estimate a blueshift of $\sim$250 km s$^{-1}$ in [O I] components at an epoch of +275 d (see Figs 5 and 8), however due to the absence of any other evidence this is not enough to claim dust formation in the SN 2008gz ejecta.

## 5 PHOTOSPHERIC AND H-ENVELOPE VELOCITIES OF EJECTA

We used the multiparametric resonance scattering code SYNOW (Branch et al. 2001, 2002; Baron et al. 2005) for modelling the spectra of SN 2008gz to interpret the spectral features and estimate the velocities of layers at different epochs. The algorithm works on the assumptions of spherical symmetry, homologous expansion of layers ($v \sim r$) and a sharp photosphere producing a blackbody spectrum and associated in the early stages with a shock wave. In the photospheric phase, the spectral lines are formed by the shell above the thick photosphere, but in the nebular phase all visible regions are optically thin (Branch et al. 2001). Each of these two phases of SN evolution can be explained with individual approximations and the modelling of the observed spectra needed in different synthetic codes.

Our main aim in modelling the spectral features is to estimate the velocities of the layers and tbe pseudo-photosphere. It was also noted in Branch et al. (2001) that there is no sharp division between the photosphere and the nebular phases. We note the presence of absorption components in the iron and hydrogen lines in the latest spectra, which can be explained as a result of the decreasing resonance-scattering mechanism. Although resonance-scattering codes like SYNOW are not used for describing late-time spectra (see for example Elmhamdi et al. 2006), we use it to

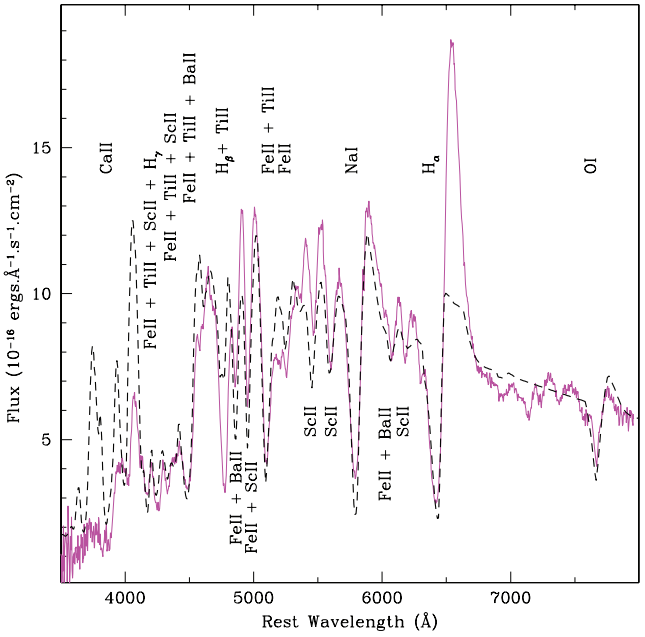


**Figure 9.** SYNOW modelling of the +87 d spectrum of SN 2008gz. The solid curve is the observed spectrum, corrected for redshift, the dashed curve is the synthetic one. The line identification is done after considering the SN as a spherically expanding fireball and lines are formed in a region moving ahead of the photosphere. The optical depth of an individual line is calculated through the 'Sobolev approximation'.

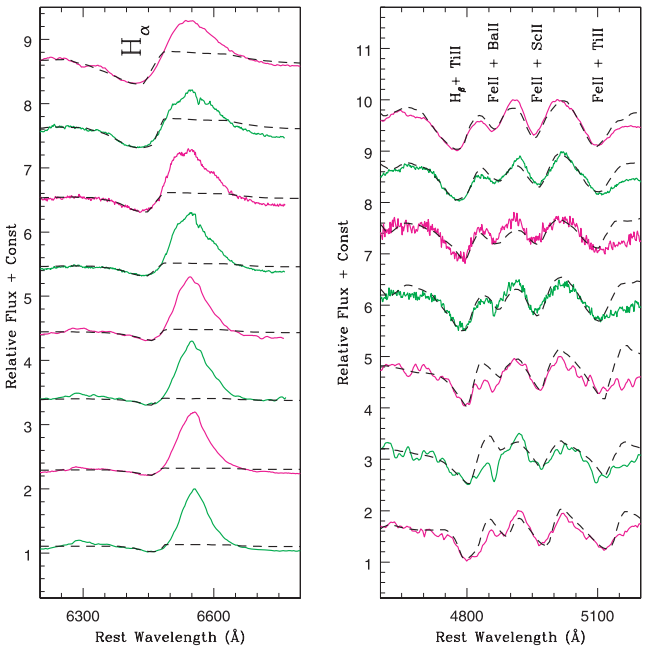


**Figure 10.** SYNOW models for absorption features of H$\alpha$ (left panel) and H$\beta$ and Fe II (right panel). The solid curves are observed spectra, corrected for redshift, the dashed curves are the synthetic spectra. The blending effect due to Sc II, T III and Ba II is also incorporated in the models. Spectral evolution corresponds (top to bottom) to +87, +115, +140, +171 +218, +222, +231 and +275 d. The H$\beta$ region is not modelled for +231 d.

describe only the absorption parts of line profiles. It is not our intention to fit the emission part of the line profiles, because this procedure needs to make use of other assumptions and other codes.

A preliminary result of the SYNOW fit for SN 2008gz is reported by Moskvitin et al. (2010). In Fig. 9, we present our model fit for the +87 d spectrum in the detached case, i.e. assuming line-forming shells of ionized gases moving ahead of the photosphere. Most of the spectral features (particularly absorption minima and the continuum) are produced well. All the identified spectral features are the same as marked in Fig. 6. We investigated undetached cases (Sonbas et al. 2008) as well, and also attempted changing density laws (exponential and power) and we found that this had very little effect while fitting the absorption minima. In order to obtain precise velocity measurements of hydrogen layers, we modelled the profiles of H$\alpha$, H$\beta$ and Fe II independently (see Fig. 10) following $\tau \sim \exp[-v(r)/v_e]$, where $\tau$ is the optical depth and $v_e$ is the e-fold velocity. We also incorporated Ti II, Sc II, and Ba II ions to model multi-minima absorption features around H$\beta$. For Fe II lines, we noticed that the velocities of various absorption features are similar or have insignificant differences and hence we used averaged Fe II values to represent the photospheric velocity ($v_{ph}$) (Branch et al. 2001; Elmhamdi et al. 2006). Estimations of photospheric and envelope velocities of different layers are given in Table 6. Uncertainties in the estimates take into account the noise in the spectra.

We also estimated photospheric and H-envelope velocities using IRAF by directly locating the absorption minima and the result is shown in Fig. 11. The velocity for Fe II 4924, 5018 and 5169 lines ranges from ~4000 km s$^{-1}$ at +87 d to around 3000 km s$^{-1}$ at +275 d. These values are similar to the values estimated above from SYNOW modelling. For H$\beta$ and H$\alpha$ layers, our values are consistently higher by about 1500 km s$^{-1}$ at all epochs than those derived from SYNOW. This discrepancy may arise due to contamination of the true absorption minima by the emission component of the P Cygni profile of H$\alpha$ and H$\beta$, and hence it is likely that the true blueshift would be overestimated while using absorption minima.

**Table 6.** Velocities of the photosphere, H$\alpha$ and H$\beta$ for different epochs of SN 2008gz evolution. All the parameters are derived from SYNOW modelling.

| UT Date (yy/mm/dd/) | Phase (days) | $v_{ph} = v$(Fe II) (km s$^{-1}$) | $v_e$(Fe II) (km s$^{-1}$) | $v$(H$\alpha$) (km s$^{-1}$) | $v_e$(H$\alpha$) (km s$^{-1}$) | $v$(H$\beta$) (km s$^{-1}$) | $v_e$(H$\beta$) (km s$^{-1}$) |
|---|---|---|---|---|---|---|---|
| 2008/11/11 | +87 | 4200 ± 400 | 1000 ± 400 | 5500 ± 200 | 2100 ± 300 | 4300 ± 300 | 1300 ± 100 |
| 2008/12/08 | +115 | 3200 ± 400 | 1500 ± 500 | 4700 ± 300 | 1500 ± 200 | 3800 ± 600 | $900^{+300}_{-100}$ |
| 2009/01/03 | +140 | 4000 ± 400 | 2500 ± 1100 | 5300 ± 400 | 1300 ± 300 | 4000 ± 400 | 1000 ± 200 |
| 2009/02/02 | +171 | 3500 ± 300 | 1600 ± 800 | 5100 ± 200 | 1300 ± 200 | 3500 ± 300 | 1000 ± 200 |
| 2009/03/22 | +218 | 3100 ± 500 | 1700 ± 900 | 4800 ± 400 | 1500 ± 500 | 3700 ± 300 | $1600^{+400}_{-800}$ |
| 2009/03/25 | +222 | 3100 ± 700 | 1200 ± 800 | $4900^{+700}_{-300}$ | $1100^{+300}_{-500}$ | 3100 ± 700 | 2000 ± 1000 |
| 2009/04/03 | +231 | <5400 | — | $4800^{+600}_{-200}$ | $1600^{+200}_{-600}$ | — | — |
| 2009/05/17 | +275 | $2000^{+200}_{-100}$ | 1500 ± 500 | 3800 ± 200 | 600 ± 200 | 2000 ± 100 | $600^{+600}_{-200}$ |

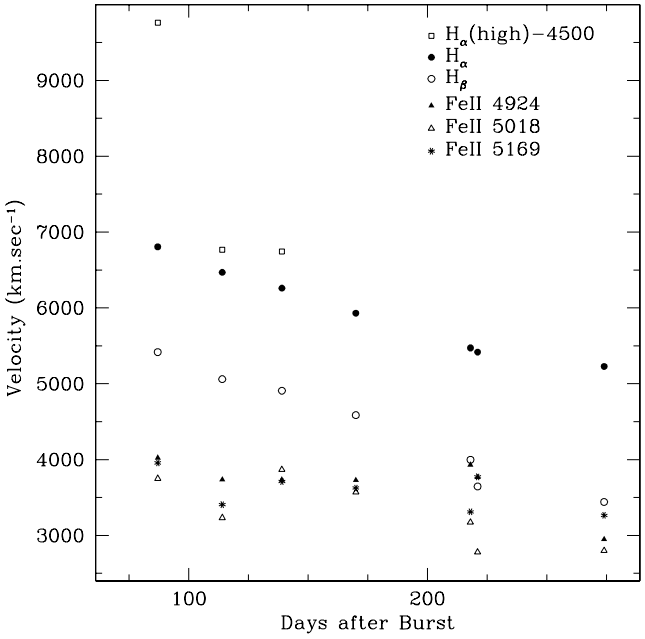


**Figure 11.** Velocity profiles of different elements in the ejecta of SN 2008gz.

For SN 2008gz, the H$\alpha$ velocity at +87 d is ∼6800 km s$^{-1}$, while for SNe 2004et it is ∼6000 km s$^{-1}$ (Sahu et al. 2006). H$\beta$ also shows a higher expansion velocity at comparable epochs. Similarly, the photospheric velocity at day +50 is ∼3700 km s$^{-1}$, while it is 4000 km s$^{-1}$ at +87 d for SN 2008gz. So, even by considering an overestimate of the plateau period by about 25 d (i.e. for $t_i \sim 95$ d), the photospheric and H-envelope velocities for SN 2008gz seem to have values comparable with or higher than those of SN 2004et. The photospheric velocity is a good indicator of the explosion energy (see Dessart et al. 2010) and hence SN 2008gz has an explosion energy similar to that of SN 2004et, ∼2.3 × 10$^{51}$ erg (Utrobin & Chugai 2009) or higher. Utrobin (2007) obtains an explosion energy of ∼1.3 × 10$^{51}$ erg for SN 1999em, which has a comparatively lower expansion velocity than SN 2004et at similar epochs.

## 6 DISTANCE AND EXTINCTION OF SN 2008GZ

The spectrum of the nuclear region of the host galaxy taken at +170 d (see Fig. 12[8]) was used to estimate $cz_{\rm helio}$, the heliocentric velocity. Employing five nebular emission lines and prominent absorption features and using the 5577-Å skyline as a reference wavelength, we obtain a $cz_{\rm helio}$ value of 1891 ± 14 km s$^{-1}$ This is in agreement with 18 other radio and optical measurements of $cz_{\rm helio}$ of NGC 3672 (in range of 1400–2000 km s$^{-1}$) listed in HyperLEDA.[9] The combined measurement gives a mean $cz_{\rm helio}$ of ∼1864 ± 19 km s$^{-1}$ and it corresponds to a corrected (Local Group infall into Virgo) distance of ∼25.65 ± 2.93 Mpc.[10] NED[11] lists four distance measurements based on the H I Tully–Fisher relation, with a mean of 25.25 ± 4.0 Mpc, which is in agreement with the above kinematic estimate; we therefore adopt an uncertainty-weighted distance of 25.5 ± 2.4 Mpc for SN 2008gz.

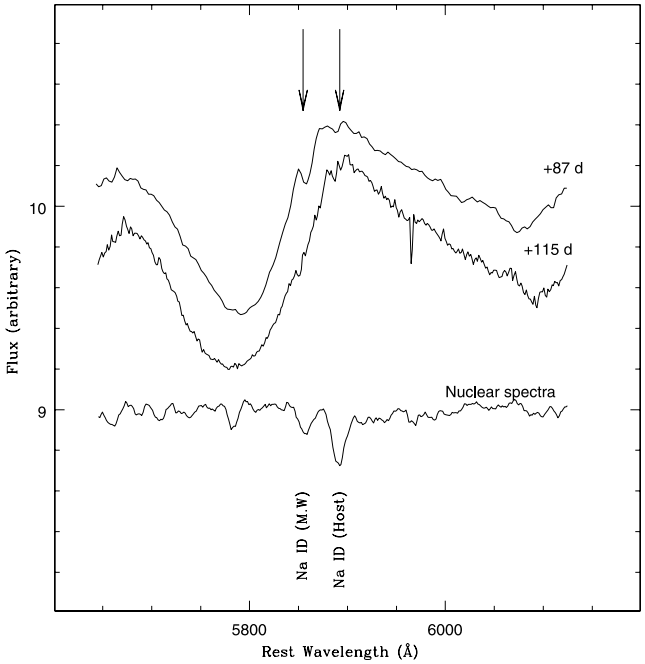


**Figure 13.** Rest-wavelength spectra of SN 2008gz (+87 d/10 Å and +115 d/6 Å) and the centre of the host galaxy (+170 d/6 Å). Na I D absorption due to interstellar matter of the host galaxy (∼5892 Å) and the Milky Way (∼5854 Å) is indicated.

**Table 7.** Equivalent-width measurements of Na I D absorption in the spectra of SN 2008gz and the host galaxy. The last row provides the uncertainty-weighted EW of Na I D absorption in the direction of SN 2008gz due to the Milky Way and the host.

| UT Date (yy/mm/dd/) | Phase (days) | EW (MW) (Å) | EW(host) (Å) |
|---|---|---|---|
| 2008/11/11 | +87 | 1.39 ± 0.34 | 0.23 ± 0.28 |
| 2008/12/08 | +115 | 1.21 ± 0.69 | 0.28 ± 0.50 |
| 2009/02/02 | +171 | 1.32 ± 1.29 | – |
| Weighted EW | | 1.29 ± 0.29 | 0.23 ± 0.24 |

The Galactic reddening in the direction of SN 2008gz as derived from the 100-μm all-sky dust-extinction map of Schlegel, Finkbeiner & Davis (1998) is estimated as $E(B-V) = 0.041 \pm 0.004$ mag. Additionally, we could also determine reddening in the direction of SN 2008gz from the equivalent widths of the Na I D absorption lines present in the spectra of SN 2008gz (+87 d and +115 d) and the centre of the host galaxy (see Fig. 13). The $D_1$ (5889.95 Å) and $D_2$(5895.92 Å) components of Na I D are not resolved in the +87 d spectra and are seen as narrow absorption features overlaid on the broad P Cygni emission wings of Na I D due to the SN. In the rest-wavelength plot the host-galaxy contribution is seen at ∼ −80 km s$^{-1}$, while the Galactic contribution is at −1630 km s$^{-1}$. In the +115 d spectrum, both components of Na I D are resolved. Intriguingly, the Galactic component appears to split into two: a stronger component at ∼ −1896 km s$^{-1}$ (due to the Milky Way ISM) and a weaker component at ∼ −1021 km s$^{-1}$, possibly due to the intergalactic medium. In the +170 d spectra, the Galactic Na I D absorption appears as a single component. Estimated total Na I D equivalent widths (EWs) are reported in Table 7.

[8] Fig. 12 is available only in electronic form – see Supporting Information.
[9] http://leda.univ-lyon1.fr/
[10] The cosmological model with $H_0 = 70$ km s$^{-1}$. Mpc$^{-1}$, $\Omega_m = 0.3$ and $\Omega_\Lambda = 0.7$ is assumed throughout the paper and the uncertainty corresponds to a local cosmic thermal velocity of 208 km s$^{-1}$ (Terry, Paturel & Ekholm 2002).
[11] http://nedwww.ipac.caltech.edu/

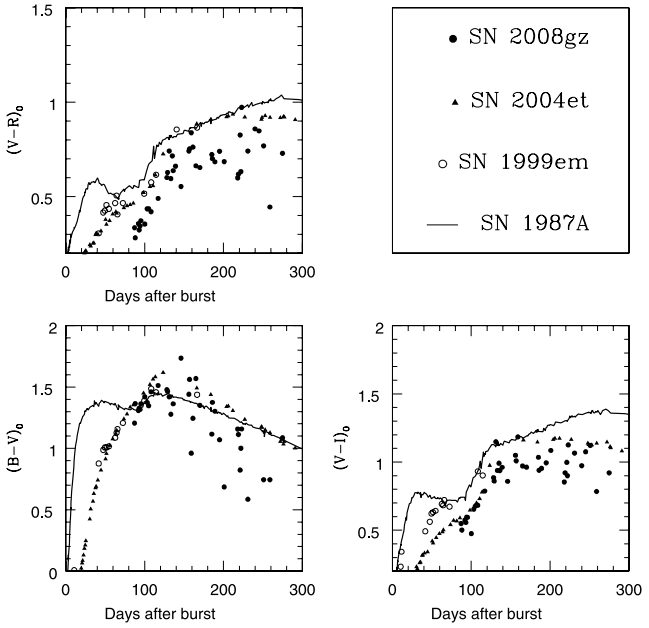


**Figure 14.** Temporal variation of colour of SN 2008gz. Also shown are other core-collapse supernovae: SN 1987A, SN 1999em and SN 2004et.

Quoted errors in EW are the photon-noise-dominated RMS uncertainties derived following Vollmann & Eversberg (2006, see their equation 6). It is seen that the EW contribution due to the host ($0.23 \pm 0.24$ Å) is smaller in comparison with the total Galactic contribution ($1.29 \pm 0.29$ Å).

It is known that the EWs of interstellar absorption bands are well correlated with the reddening $E(B-V)$ estimated from the tail of SNIa colour curves (Barbon et al. 1990; Richmond et al. 1994) and by employing the empirical relation established by Turatto, Benetti & Cappellaro (2003), $E(B-V) = -0.01 + 0.16$ EW (where EW is in Å),[12] we obtain the Galactic $E(B-V)$ contribution as $0.20 \pm 0.05$ mag and that of the host galaxy as $0.03 \pm 0.04$ mag. The Galactic $E(B-V)$ derived in this way is larger than that derived from a Schlegel map. Considering the normal extinction law ($R_V = 3.1$) and a Schlegel value of $E(B-V) = 0.041$ for the Milky Way, the EW (host/Galactic) ratio would suggest a slightly lower reddening in the host ($E(B-V) \leq 0.01$ mag). However, the host-galaxy value of 0.03 mag may not be ruled out in the case of a different dust-to-gas ratio for the host.

For this work, we will adopt a conservative value of $E(B-V) = 0.07 \pm 0.04$ mag, obtained by adding the Galactic (Schlegel) and host galaxy (Na I D) contributions. This corresponds to a visual extinction ($A_V$) of $0.21 \pm 0.12$ by assuming a ratio of total-to-selective extinction $R_V = 3.1$ (Cardelli, Clayton & Mathis 1989).

## 7 TEMPORAL EVOLUTION OF COLOUR AND BOLOMETRIC LUMINOSITY

Fig. 14 shows the reddening-corrected colour evolution of SN 2008gz. For comparison, we also show the reddening-corrected colour curves of SN 1987A (Suntzeff & Bouchet 1990), SN 1999em (Elmhamdi et al. 2003a) and SN 2004et (Sahu et al. 2006) for $E(B-V)$ of 0.15, 0.10 and 0.41 mag and explosion epochs of JD 244 6849.82, 245 1480.5 and 245 3275.5 respectively. Though the colour curves of SN 2008gz have large scatter, the overall nature of its temporal evolution is prominent. SN 2008gz follows the general trend of colour evolution, i.e. a steep and rapid decrease from blue (high temperature) to red (low temperatures) colours similar to SNe 2004et and 1999em. $(B-V)_0$ becomes redder from 1.2 mag at +87 d to about 1.7 mag at +140 d and it follows a trend similar to SNe 2004et and 1999em. The overall trend in the colour evolution of SN 2008gz between the end of plateau and middle of the tail is similar to that of the peculiar Type II SN 1987A. In the nebular phase, $(B-V)_0$ turns blue rather rapidly, $-1$ mag $(100\,\mathrm{d})^{-1}$, and this arises due to suspected flattening in the $B$ light and a shallow decay in $V, R$ and $I$ bands. The $(V-R)_0$ colour is found to be consistently bluer than for other IIP SNe. For $(V-R)_0$ and $(V-I)_0$, the increment is quite shallow during the transition from plateau to nebular phases. This is in contrast to the colour evolution of low-luminosity Type II peculiar SNe 1997D and 1999eu, where a steep rise and excess in colour has been noticed (Pastorello et al. 2004; Misra et al. 2007).

Bolometric luminosity is essential to estimate the total optical radiant energy in the explosion and during the tail phase it is also a good estimator of radioactive $^{56}$Ni synthesized in the explosion. To a good approximation, the integration of extinction-corrected flux in *UBVRI* at a given epoch gives a meaningful estimate of bolometric luminosity. The extinction-corrected *BVRI* magnitudes were converted into fluxes using zero-points given by Bessell, Castelli & Plez (1998) and the total *BVRI* flux is obtained by interpolating and integrating fluxes between 0.4 and 0.85 μm. Fig. 15 shows the percentage flux contribution in different passbands and the overall trend is found to be similar to that of SN 1987A. From plateau (+87 d) to nebular (+140 d) phases, the flux contribution declines from ∼15–10 per cent in $B$ and from ∼25–20 per cent in $V$, while it ascends from ∼36–42 per cent in $R$ and from ∼22–30 per cent in $I$. In the nebular phase (until +270 d), the flux contributions remain constant. For nearby SNe 1987A and 2004et, large (∼40 per cent)

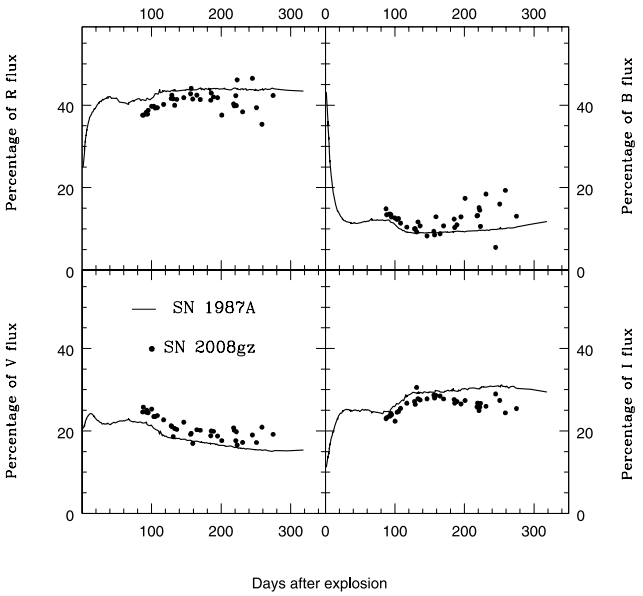


**Figure 15.** Flux contribution, in percentage, of the *BVRI* bands of SN 2008gz, along with a comparison with SN 1987A.

[12] In Turatto, Benetti & Cappellaro (2003) there are two relations: one is with low slope and the other with a high slope. In this work we have considered the lower slope, because it is well sampled and matches with previous works in this area (Barbon et al. 1990).

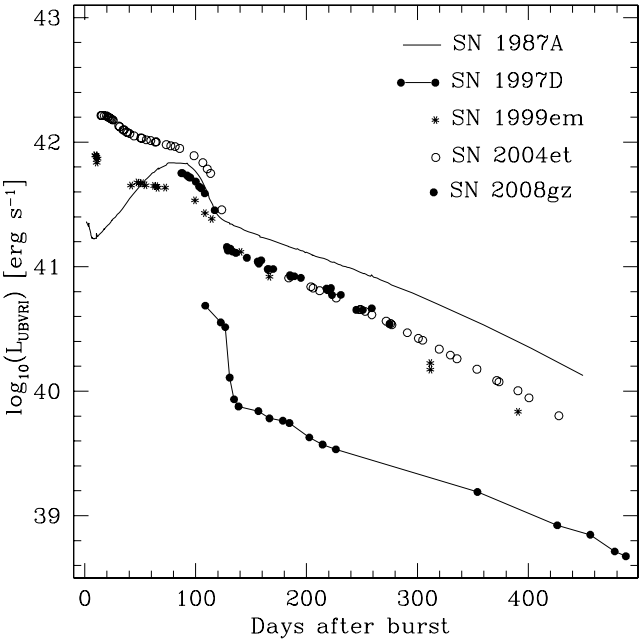


**Figure 16.** Bolometric light curve of SN 2008gz. For comparison, we also show light curves of SN 1987A, SN 1997D, SN 1999em and SN 2004et.

flux contributions in the *U* and *B* bands are observed in the initial epochs, which reduce to a few percent by +60 d. Towards later epochs, however, when the SN ejecta become optically thin, a little enhancement (about 5 per cent) in *U* and *B* bands is also noticeable (Misra et al. 2007). Therefore, for SN 2008gz, we have constructed a *UBVRI* bolometric light curve after making a constant (5 per cent) contribution from the *U* band over the period of our observation. No correction for flux contributions in the ultraviolet and near-infrared regions was made, as they become significant respectively in the early and late phases of the light curve evolution.

Fig. 16 shows the *UBVRI* bolometric nature of SN 2008gz along with other Type II events. The different behaviour of these events is clearly evident and it provides a constraint on the synthesized radioactive $^{56}$Ni as well as the explosion energy of SNe. The tail luminosity of SN 2008gz is similar to that of SN 2004et, while the plateau luminosity is about 0.2 dex fainter. Explosion parameters for SN 2008gz are estimated in the next sections.

## 8 PHYSICAL PARAMETERS

### 8.1 Amount of ejected radioactive nickel

The nebular-phase light curve of Type II SNe is mainly governed by the radioactive decay of $^{56}$Ni to $^{56}$Co to $^{56}$Fe, which have a half-life of 6.1 and 111.26 d respectively, and hence the tail luminosity is directly proportional to the amount of $^{56}$Ni synthesized by explosive burning of Si and O during shock breakout (Arnett 1980; Arnett 1996).

By using the tail luminosity, the $^{56}$Ni mass can be derived following the method described by Hamuy (2003) applied under the assumption that all the $\gamma$-rays emitted during radioactive decay make the ejecta thermalized. For SN 2008gz using the *V*-band magnitude at +200 d corrected for extinction ($A_V = 0.21 \pm 0.12$ mag; Section 6), a bolometric correction of $0.26 \pm 0.06$ mag (Hamuy 2001) during the nebular phase and a distance modulus of $32.03 \pm 0.21$, we derive a tail luminosity of $1.51 \pm 0.29 \times 10^{41}$ erg s$^{-1}$ and this, for the plateau duration of 115 d, results in a Ni mass $M_{\rm Ni} = 0.067 \pm 0.012$ M$_\odot$.

We can estimate the mass of $^{56}$Ni by a direct comparison with SN 1987A, for which it is accurately determined as 0.075 M$_\odot$. We note that the temporal evolution of the flux contribution in different bands for SN 2008gz is comparable with that for SN 1987A (Section 7) and consequently we can safely assume that at a comparable epoch the ratio of their luminosities is equal to the ratio of synthesized $^{56}$Ni mass. SN 2008gz attains the deep nebular phase beyond 150 d after the burst. The last observation was also performed at nearly +275 d. Hence, the mean ratio between the tail *UBVRI* bolometric luminosity of SN 2008gz (∼150–275) and that of SN 1987A is about 0.539. This implies for SN 2008gz an ejected $^{56}$Ni mass [$0.539 \times 0.075$] ≈ 0.041 M$_\odot$.

By taking a sample of ten IIP SNe, Elmhamdi et al. (2003b) show that the steepness of the *V*-band light-curve slope (defined as $S = {\rm d}m_V/{\rm d}t$) at the inflection time ($t_i$) is anticorrelated with the $^{56}$Ni mass ($\log M_{\rm Ni} = -6.2295\ S - 0.8147$). For SN 2008gz we have a well-sampled transition phase and obtain a value of $S = 0.075 \pm 0.036$ mag d$^{-1}$ (see Fig. 17[13]), which corresponds to $M_{\rm Ni} = 0.052 \pm 0.01$ M$_\odot$. Considering the uncertain values of extinction towards SN 2008gz, we note that for SNe 2004A and 2003gd Hendry et al. (2006) find that the Elmhamdi et al. (2003b) scheme gives somewhat lower values. Further, based on plateau luminosity, the linear correlation $\log M_{\rm Ni} = -0.438\ M_V(t_i - 35) - 8.46$ found by Elmhamdi et al. (2003b) provides a value of $^{56}$Ni mass of 0.051 M$_\odot$ for an $M_V$ of $-16.37 \pm 0.24$ at +87 d ($t_i - 28$). Taking the average of the above four estimates, we obtain the amount of produced $^{56}$Ni mass = $0.05 \pm 0.01$ M$_\odot$. For estimation of other physical quantities, we assume that the above amount of $^{56}$Ni was produced by SN 2008gz. However, we should point out that adopting a smaller plateau duration (Section 2.2) will reduce the amount of ejected radioactive $^{56}$Ni, which will further propagate in the determination of progenitor properties (Section 8.3).

### 8.2 Environment of the progenitor

Constraints on the nature of progenitors of core-collapse SNe are derived from study of the environments in which they occur. For example, by correlating the position of explosion sites with the sites of recent star formation as traced by H$\alpha$ line emission, it is found (see e.g. James & Anderson 2006; Anderson & James 2008; Kelly, Krishner & Pahre 2008) that core-collapse events are excellent tracers of star formation, and Type Ib/c are more likely to be associated with regions of high surface brightness or high H$\alpha$ emission than Type II SNe. Anderson & James (2009) found that Type IIP events are likely to be more centrally concentrated than other II subtypes. SN 2008gz occurred in the spiral arm of the host galaxy at a deprojected galactocentric distance of 2.8 kpc (within the half-light radius) and the oxygen abundance ([O/H] = $12 + \log N_{\rm O}/N_{\rm H}$) of the galactic ISM at the position of the SN is estimated as 8.6 (derived from the O/H-$M_{\rm B}$ relation proposed by Pilyugin, Vílchez & Contini 2004), which is close to the solar abundance for [O/H] of 8.65 (Asplund et al. 2009).

In order to investigate the level of H$\alpha$ emission further, we observed NGC 3672 in the narrow-band H$\alpha$ line ($\lambda_c = 6551$ Å) and H$\alpha$ red ($\lambda_c = 6650$ Å), which have FWHM of 83 and 79 Å respectively. We used a 2k CCD camera mounted on the 1-m ST, Nainital on 2010 February 18 (+560 d). A total exposure of 1 h in H$\alpha$-line and

[13] Fig. 17 is available only in electronic form – see Supporting Information.

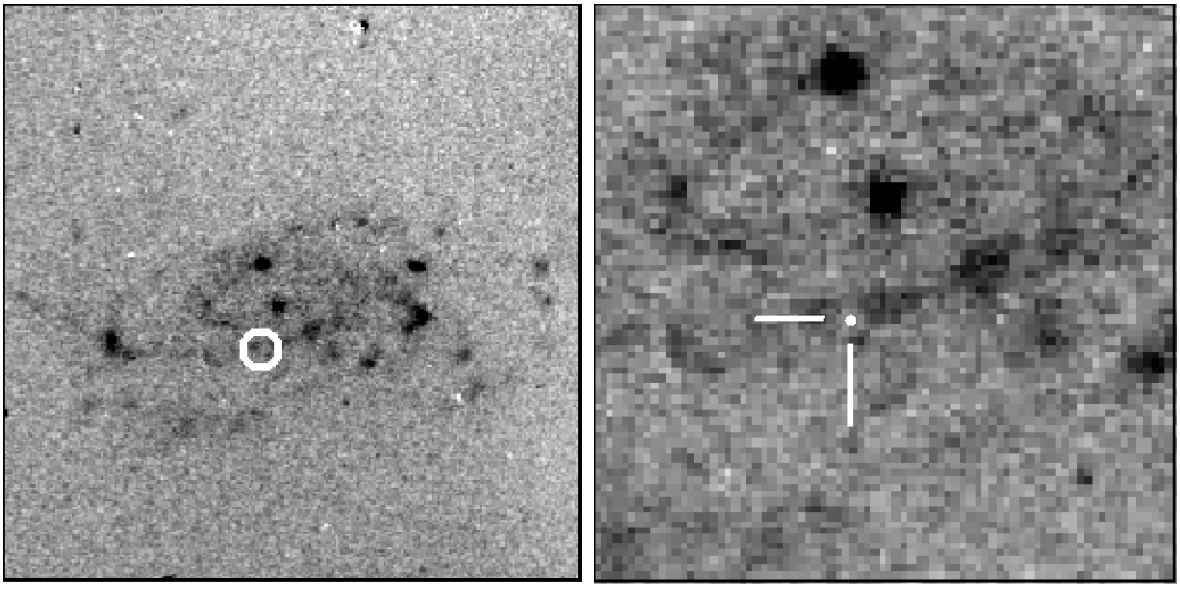

**Figure 18.** Continuum-subtracted H$\alpha$ image of NGC 3672. In the left panel ($\sim$3 $\times$ 3 arcmin$^2$) five bright H II regions are visible. The SN position is marked with a circle. In the right panel ($\sim$1 $\times$ 1 arcmin$^2$) a zoomed-in image of the SN is shown. The SN location is marked with a dot.

H$\alpha$-red filters was taken, along with several bias and sky flats. Raw images were corrected for bias and flats using IRAF. The FWHM of the stellar PSF (seeing) varied from 1.8–2.2 arcsec. Images were combined to improve the signal-to-noise ratio and continuum subtraction was performed using ISIS. Our narrow-band filter-set was not customized for extragalactic work, and we expected H$\alpha$ red to contain emission-line fluxes, since at the redshifted wavelength ($\sim$41 Å at H$\alpha$) of NGC 3672 the H$\alpha$-red filter had transmissions of 25, 40 and 80 per cent respectively for N II 6548 Å, H$\alpha$ and N II 6589 Å. We could verify this by subtracting the H$\alpha$-line frame from the broad-band *R* and *V* frames of SN taken on 2010 February 14, which gave no residual while the H$\alpha$-red frame showed residuals. Fig. 18 shows the continuum-subtracted image of SN 2008gz, revealing contributions from H$\alpha$+N II emission. A close-up view of the SN location is also shown. The sky is at a level of 0 while the peak flux is around 22 counts. Five prominent regions of H$\alpha$ emission having peak counts above 15 are clearly apparent. The SN 2008gz position is at a level of 8 counts, and hence it belongs to a low-luminosity H II region. This is also evident from the early epoch spectra, in which an emission peak (not so prominent) of zero velocity is seen.

### 8.3 Properties of the progenitor star

Accurate estimates of explosion parameters require detailed hydrodynamical modelling of the optical light curves, though analytical relations (based on a few well-modelled IIP events) correlating the physical parameters – explosion energy, pre-SN radius and total ejected mass – on the one hand and observable quantities – plateau duration, mid-plateau *V*-band magnitude $(M_V)_{\rm mp}$ and mid-plateau photospheric velocity $v_{\rm mp}$ – on the other hand are proposed to exist (see e.g. Litvinova & Nadyozhin 1985; Popov 1993; Nadyozhin 2003). For SN 2008gz, we can only provide an approximation of these observables. Estimates of $(M_V)_{\rm mp}$ and $v_{\rm mp}$ can be made using the $^{56}$Ni mass estimate and employing the following empirical relations derived (by minimizing of least squares) from the data given in Hamuy (2003, see their figs 3 and 4):

$$(M_V)_{\rm mp} = -2.597 \times \log(M_{\rm Ni}) - 20.127,$$

$$\log(v_{\rm mp}) = 0.361 \times \log(M_{\rm Ni}) + 4.123.$$

For $M_{\rm Ni} = 0.05 \pm 0.01$ M$_\odot$, we derive $(M_V)_{\rm mp} = -16.7^{-0.2}_{+0.3}$ mag and $v_{\rm mp} = 4503^{+306}_{-348}$ km s$^{-1}$. This value of absolute magnitude is consistent with those obtained from the first photometric *V* point (Section 9). These estimates, along with a plateau duration of 115 d, provide (Litvinova & Nadyozhin 1985) a burst energy $\sim 2.5^{+0.8}_{-0.7} \times 10^{51}$ erg, ejected mass $\sim 34^{+10}_{-8}$ M$_\odot$ and pre-SN radius $\sim 167^{+106}_{-61}$ R$_\odot$. The explosion energy derived in this way is consistent with the one expected from the photospheric velocity (see Section 5); however, the ejecta mass is larger in comparison to the typical progenitor mass range (8.5–16.5 M$_\odot$) estimate derived from pre-explosion SN images (Smartt et al. 2009) and this may be due to uncertainty in the above-measured parameters.

Dessart et al. (2010) demonstrate that by employing the explosion-energy estimate, the observed line width of [O I] and artificially generated radiation hydrodynamic simulations of core-collapse SNe, it is possible to put an upper limit on the main-sequence mass of the progenitor. For SN 2008gz, the oxygen ejecta velocity of $\sim$1250 km s$^{-1}$ (HWHM of the [O I] profile, see Section 4, which is slightly higher than $\sim$1000 km s$^{-1}$ observed for SNe 2004et and 1999em at around +330 d) and the assumption of an explosion energy of 3 $\times$ 10$^{51}$ erg s$^{-1}$ provide a main-sequence mass of 15 (12) M$_\odot$ respectively for non-rotating (rotating) pre-SN models, while assuming an ejecta velocity of 1500 km s$^{-1}$ for [O I] gives an upper limit of 17(13) M$_\odot$, which is consistent with that derived using pre-explosion images (Smartt et al. 2009).

## 9 COMPARISON WITH OTHER CORE-COLLAPSE SUPERNOVAE

A detailed investigation of SN 2008gz indicates that it is a normal Type IIP event showing photometric and spectroscopic evolution similar to archetypal SNe 2004et and 1999em. SN 2008gz occurred in a highly inclined ($\Theta_{\rm inc} = 56\overset{\circ}{.}2$) host galaxy, within a

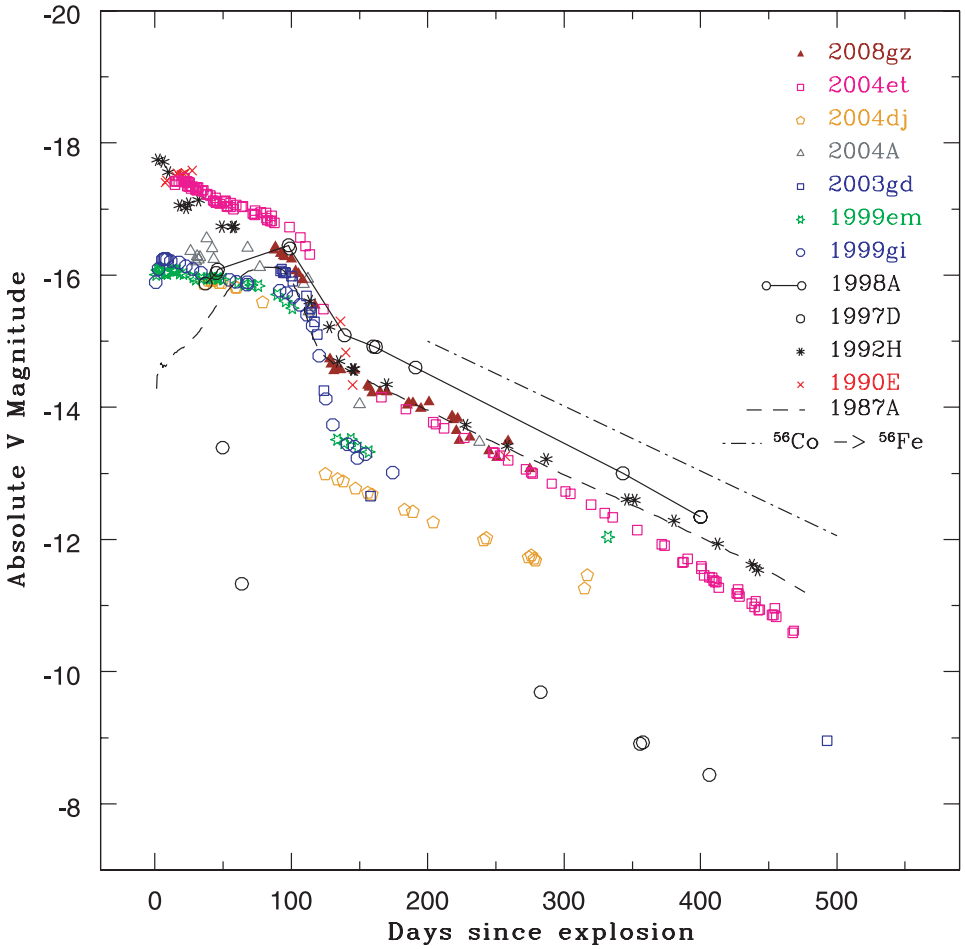


**Figure 19.** Comparison of the absolute $V$-band light curve of SN 2008gz with other Type IIP SNe: SN 2004et, SN 2004dj, SN 2004A, SN 2003gd, SN 1999em, SN 1999gi, SN 1998A, SN 1997D, SN 1992H, SN 1990E and SN 1987A. The magnitudes have been corrected for distance and readdening.

deprojected galactocentric radius of $0.27r_{25}$ (Table 1), implying a solar-metallicity region similar to SNe 1999em and 2005cs, though its explosion and other properties were found to be similar to SN 2004et, which occurred on the outskirts of its host galaxy. Our narrow-band H$\alpha$ photometry indicates that SN 2008gz was associated with a star-forming low-luminosity H II region of the galaxy. Thus, the metallicity appears to have little effect on the explosion properties of core-collapse SNe.

In Fig. 19 we show the absolute $V$-band light curve of well studied core-collapse events collected from the literature (see Misra et al. 2007, for references). The plateau luminosity ($M_V \sim -16.6$)[14] of SN 2008gz is at a similar level to those for peculiar SNe 1987A, 1998A and it lies between the brighter end of IIP SNe 1990E, 1992H, 2004et ($\sim -17$ mag) and the fainter end of SN 1997D ($\sim -15$ mag). This shows that SN 2008gz is a normal event, both in energetics and nickel production. These values of plateau luminosity for IIP SNe are lower than $-17.6 \pm 0.6$ mag, which was predicted using theoretical models calculated by Höflich et al. (2001) for IIP SNe based on a wide range of parameters (explosion energy, metallicity, mass loss of progenitor).

[14] We estimate the value of mid-plateau $M_V$ as $-16.6 \pm 0.2$ mag; by considering an average decline rate of 0.006 mag d$^{-1}$ during the plateau phase of SNe 1999em and 2004et, we found that the mid-plateau magnitude of SN 2008gz was $\sim$0.2 mag brighter than that determined at +87 d (Section 8.1). We assume an $A_V$ of 0.214 mag.

SN 2008gz showed a rarely observed 1.5-mag drop in $V$ from plateau to nebular phases and it had a tail luminosity comparable to (or higher than) SN 2004et, resulting in a synthesized $^{56}$Ni mass in range 0.05–0.1 M$_\odot$. The large tail luminosity of SN 1998A indicates that the thermalization process for 1998A was more efficient than that for SN 2008gz. The colour evolution of SN 2008gz has a similar trend to normal IIP and peculiar SNe 1987A and 1998A. The expansion velocity of the SN 2008gz ejecta was comparable to that of SN 2004et or higher, implying an explosion energy of $\sim 2 \times 10^{51}$ erg. Our calculation for the progenitor mass (Section 8.3) of SN 2008gz favours a mass range of 13–18 M$_\odot$ (i.e. SNe 1999em, 1999gi, 2004dj, 2004et) over a lower mass range of 8–18 M$_\odot$ (i.e. SNe 1997D, 2004A, 2005cs). This progenitor mass grouping is also favoured on the basis of radio luminosity (Chevalier, Fransson & Nymark 2006). As an alternative scenario, SN 2008gz can be characterized as a peculiar event. Lack of data in the first 1–2 months after the explosion and spectral similarity with SN 1998A (Benetti et al. 2008) also indicate the possibility that SN 2008gz is a peculiar Type II event. Fig. 20 shows a comparison of the spectrum of SN 2008gz with those of SN 2004et and SN 1998A at a comparable epoch. There are many similarities between the spectral features of SN 2008gz and SN 1998A. On the other hand, low rates of peculiar Type II SN, similarity in the late light curve of SN 2008gz and Type IIP events and the similarity of some particular spectral features, like the high-velocity H$\alpha$ line (Section 4), of this event with SNe 2004et and

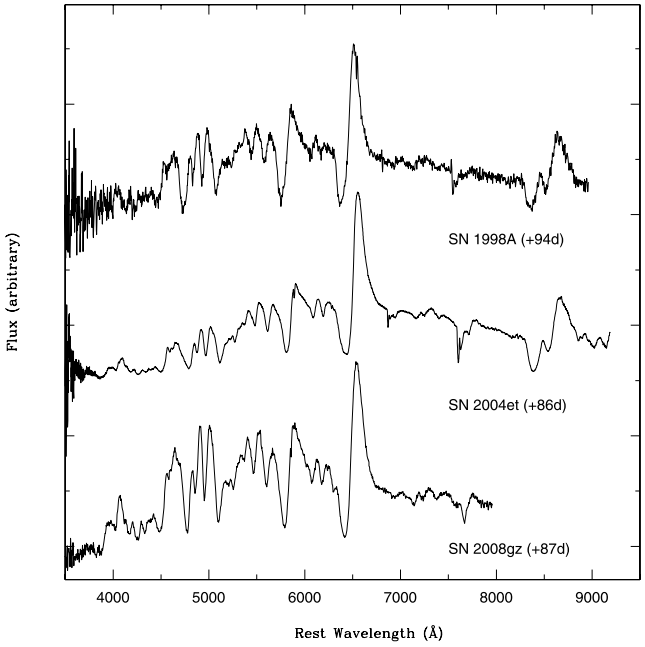


**Figure 20.** Comparison of the spectral features of SN 2008gz with those of SN 2004et and SN 1998A.

1999em also indicate that SN 2008gz should be a normal Type IIP event.

## 10 SUMMARY

We present *BVRI* photometric and low-resolution spectroscopic observations of a supernova event SN 2008gz which occurred in a spiral arm and within the half-light radius of nearby (∼25 Mpc) galaxy NGC 3672. As the event was buried in the galaxy light, we used a template-subtraction technique to estimate the apparent magnitude of the event. We monitored the event for a period of ∼200 d. We summarize our results as follows.

(i) The photometric and spectral nature of the event indicate similarity to normal Type IIP SNe 2004et and 1999em. The event was discovered by about 82 d after the burst, and has a plateau phase that lasted 115 ± 5 d. We monitored the SN evolution from +87 d to +275 d.

(ii) We estimate the photospheric and H-envelope velocity using both direct measurements of the absorption minima of H I and Fe II lines and SYNOW modelling of the spectra. Here both values agree well within the uncertainties. We estimate a photospheric velocity of ∼4000 km s$^{-1}$ at +87 d, which is higher than that observed for the well-studied SN 2004et at similar epochs, indicating an explosion energy comparable to or higher than that of 2004et. A similar trend was also seen for the expansion velocity of H envelopes.

(iii) Using the pre-SN models of Dessart et al. (2010) and also by comparing explosion energies (derived by using hydrodynamical models) of well-studied IIP SNe, we find that SN 2008gz had an explosion energy of 2–3 × $10^{51}$ erg s$^{-1}$. This estimation, coupled with the observed width of the forbidden [O I] line, gives an upper limit for the main-sequence progenitor mass of 17 $M_{\odot}$.

(iv) SN2008gz exhibits a rarely observed drop of 1.5 mag within 30 d in the *V*-band from plateau to nebular phases; this is higher than the typically observed fall of 2–3 mag in normal IIP SNe. Adopting $A_V = 0.21$ mag, we can estimate the mass of $^{56}$Ni synthesized during the explosion as 0.05 ± 0.01 $M_{\odot}$.

(v) Our H$\alpha$ observation taken about 560 d after the explosion indicates that the event took place in a low-luminosity star-forming arm, very close to a H II region. The emission kink of this H II region is also seen in the H$\alpha$ line near zero velocity of the Doppler-corrected spectra of the SN.

## ACKNOWLEDGMENTS

We are thankful to the reviewer Stefano Valenti for his valuable comments, which have enriched the manuscript. We thank all the observers at Aryabhatta Research Institute of Observational Sciences (ARIES), who provided their valuable time and support for observations of this event. We are thankful to the observing staff of the 2-m IGO, 3.6-m TNG, 3.6-m NTT and 6-m BTA for their kind cooperation in observation of SN 2008GZ. We also express our thanks to the observing staff of Perth Observatory for their kind support for this research work. This work was supported by the grant RNP 2.1.1.3483 of the Federal Agency of Education of Russia. TAF and ASM were supported by a grant of the President of the Russian Federation (MK-405.2010.2). This work is partially based on observations made with the Italian Telescopio Nazionale Galileo (TNG) operated on the island of La Palma by the Fundación Galileo Galilei of the INAF (Istituto Nazionale di Astrofisica) at the Spanish Observatorio del Roque de los Muchachos of the Instituto de Astrofisica de Canarias. It is also partially based on observations collected at the European Southern Observatory, Chile under the program 083.D-0970(A). SB and MFB are partially supported by the PRIN–INAF 2009 with the project 'Supernovae Variety and Nucleosynthesis Yields'. This research has made use of data obtained through the High Energy Astrophysics Science Archive Research Center Online Service, provided by the NASA/Goddard Space Flight Center. We are indebted to the Indo-Russian (DST-RFBR) project No. RUSP-836 (RFBR-08-02:91314) for the completion of this research work.

## REFERENCES

Alard C., Lupton R. H., 1998, ApJ, 503, 325
Anderson J. P., James P. A., 2008, MNRAS, 390, 1527
Anderson J. P., James P. A., 2009, MNRAS, 399, 559
Andrews J. E. et al., 2010, ApJ, 715, 541
Arnett W. D., 1980, ApJ, 237, 541
Arnett W. D., 1996, Supernovae and Nucleosynthesis. Princeton Univ. Press, Princeton, NJ
Asplund M., Grevesse N., Sauval A. J., Scott P., 2009, ARA&A, 47, 481
Barbon R., Benetti S., Rosino L., Cappellaro E., Turatto M., 1990, A&A, 237, 79
Baron E., Nugent P. E., Branch D., Hauschildt P. H., 2005, in Turatto M., Benetti S., Zampieri L., Shea W., eds, ASP Conf. Ser. Vol. 342, Supernovae as Cosmological Lighthouses. Astron. Soc. Pac., San Francisco, p. 351
Benetti S. et al., 2001, MNRAS, 322, 361
Benetti S., Boschin W., Harutyunyan H., 2008, Cent. Bur. Electron. Telegrams, 1568, 1
Bessell M. S., Castelli F., Plez B., 1998, A&A, 333, 231
Branch D., Baron E., Jeffery D. J., 2001, in Weiler K., ed., Supernovae and Gamma-Ray Bursters, Lecture Notes in Physics 598. Springer-Verlag, Berlin, p. 47
Branch D. et al., 2002, ApJ, 566, 1005
Cappellaro E., Danziger I. J., della Valle M., Gouiffes C., Turatto M., 1995, A&A, 293, 723
Cappellaro E., Evans R., Turatto M., 1999, A&A, 351, 459
Cardelli J. A., Clayton G. C., Mathis J. S., 1989, ApJ, 345, 245

Chakraborty P., Das H. K., Tandon S. N., 2005, Bull. Astron. Soc. India, 33, 1
Chevalier R. A., Fransson C., Nymark T. K., 2006, ApJ, 641, 1029
Chugai N., 1988, Sov. Astron. Lett., 14, 334
Danziger I. J., Lucy L. B., Bouchet P., Gouiffes G., 1991, in Woosely S. E., ed., Supernovae. Springer, New York, p. 69
Dessart L., Livne E., Waldman R., 2010, MNRAS, 408, 827
Elmhamdi A. et al., 2003a, MNRAS, 338, 939
Elmhamdi A., Chugai N. N., Danziger I. J., 2003b, A&A, 404, 1077
Elmhamdi A., Danziger I. J., Branch D., Liebundgut B., Baron E., Kirshner R. P., 2006, A&A, 450, 305
Filippenko A. V., 1997, ARA&A, 35, 309
Gupta R., Burse M., Das H. K., Kohok A., Ramprakash A. N., Engineer S., Tandon S. N., 2002, Bull. Astron. Soc. India, 30, 785
Gurugubelli U. K., Sahu D. K., Anupama G. C., Chakradhari N. K., 2008, Bull. Astron. Soc. India, 36, 79
Habergham S. M., Anderson J. P., James P. A., 2010, ApJ, 717, 342
Hakobyan A. A., Mamon G. A., Petrosian A. R., Kunth D., Turatto M., 2009, A&A, 508, 1259
Hamuy M., 2001, PhD thesis, Univ. Arizona
Hamuy M., 2003, ApJ, 582, 905
Hamuy M., Pinto P. A., 2002, ApJ, 566, 63
Hamuy M., Suntzeff N. B., Heathcote S. R., Walker A. R., Gigoux P., Phillips M. M., 1994, PASP, 106, 566
Hanuschik R. W., Dachs J., 1987, A&A, 182, L29
Harutyunyan A. H. et al., 2008, A&A, 488, 383
Heger A., Fryer C. L., Woosley S. E., Langer N., Hartmann D. H., 2003, ApJ, 591, 288
Hendry M. A. et al., 2006, MNRAS, 369, 1303
Höflich P., Straniero O., Limongi M., Dominguez I., Chieffi A., 2001, Rev. Mex. Astron. Astrofís., 10, 157
Horne K., 1986, PASP, 98, 609
James P. A., Anderson J. P., 2006, A&A, 453, 57
Kelly P. L., Krishner R. P., Pahre P., 2008, ApJ, 687, 1201
Kumar B., Sagar R., Rautela B. S., Srivastava J. B., Srivastava R. K., 2000, Bull. Astron. Soc. India, 28, 675
Landolt A. R., 2009, AJ, 137, 4186
Leonard D. C., Filippenko A. V., Gates E. L., 2002, PASP, 114, 35
Li W., Van Dyk S. D., Filippenko A. V., Cuillandre J.-C., 2005, PASP, 117, 121
Litvinova I. Y., Nadyozhin D. K., 1985, Sov. Astron., 11, 145L
Lucy L. B., Danziger I. J., Gouiffes G., Bouchet P., 1991, in Woosely S.E., ed., Supernovae. Springer, New York, p. 82
Matheson T. et al., 2000, AJ, 120, 1487
Misra K., Pooley D., Chandra P., Bhattacharya D., Ray A. K., Sagar R., Lewin Walter H. G., 2007, MNRAS, 381, 280
Moskvitin A. S., Fatkhullin T. A., Sokolov V. V., Komarova V. N., Drake A. J., Roy R., Tsvetkov D. Yu., 2010, Astrophys. Bull., 65, 230
Nadyozhin D. K., 2003, MNRAS, 346, 97
Nakano S., Martin R., 2008, Cent. Bur. Electron. Telegrams, 1566, 1
Olivares E. F. et al., 2010, ApJ, 715, 833
Pastorello A. et al., 2004, MNRAS, 347, 74
Pastorello A. et al., 2005, MNRAS, 360, 950
Pastorello A. et al., 2009, MNRAS, 394, 2266
Pilyugin L. S., Vílchez J. M., Contini T., 2004, A&A, 425, 849
Popov D. V., 1993, ApJ, 414, 712
Poznanski D. et al., 2009, ApJ, 694, 1067
Richmond M. W., Treffers R. R., Filippenko A. V., Paik Y., Leibundgut B., Schulman E., Cox C. V., 1994, AJ, 107, 1022
Sahu D. K., Anupama G. C., Srividya S., Muneer S., 2006, MNRAS, 372, 1315
Schlegel D. J., Finkbeiner D. P., Davis M., 1998, ApJ, 500, 525
Smartt S. J., 2009, ARA&A, 47, 63
Smartt S. J., Eldridge J. J., Crockett R. M., Maund J. R., 2009, MNRAS, 395, 1409
Smith N., Li W., Filippenko A. V., Chornock R., 2011, MNRAS, 412, 1522
Sonbas E. et al., 2008, Astrophys. Bull., 63, 228
Spyromilio J., 1991, MNRAS, 253, 25
Stetson P. B., 1987, PASP, 99, 191
Stetson P. B., 1992, J. R. Astron. Soc. Can., 86, 71
Suntzeff N. B., Bouchet P., 1990, AJ, 99, 650
Suntzeff N. B., Hamuy M., Martin G., Gomez A., Gonzalez R., 1988, AJ, 97, 1864
Taubenberger S. et al., 2009, MNRAS, 397, 677
Terry J. N., Paturel G., Ekholm T., 2002, A&A, 393, 57
Turatto M., Cappellaro E., Benetti S., Danziger I. J., 1993, MNRAS, 265, 471
Turatto M. et al., 1998, ApJ, 498, L129
Turatto M., Benetti S., Cappellaro E., 2003, in Hillebrandt W., Weibundgut B., eds, From Twilight to Highlight: The Physics of Supernovae. Springer-Verlag, Berlin, p. 200
Utrobin V. P., 2007, A&A, 461, 233
Utrobin V. P., Chugai N. N., 2009, A&A, 506, 829
van Dokkum P. G., 2001, PASP, 113, 1420
Vollmann K., Eversberg T., 2006, Astron. Nachr., 327, 862

## SUPPORTING INFORMATION

Additional Supporting Information may be found in the online version of this article:

**Table 2.** Journal of photometric observation of SN 2008gz.
**Fig. 3.** Comparison of ISIS-derived magnitudes and ours for *BVRI*.
**Fig. 8.** Two-component Gaussian fit of [O I] 6300, 6364 Å emission lines. Measurements of their relative intensities quantifies whether the corresponding line-emitting region is optically thick or thin.
**Fig. 12.** Spectrum of the nucleus of the host galaxy NGC 3672 taken with the 2-m IGO. The spectrum shows H$\alpha$, N II (6548 Å and 6583 Å), and S II (6717 Å and 6730 Å) lines in emission (similar to Sc spiral galaxies), which can arise from a gaseous component heated by the AGN, post-AGB stars, shocks or cooling flows. The Ca II (K and H), H$\gamma$, H$\beta$, Mg I T, Fe I (5270 Å) and Na I D due to the Milky Way and the host are seen in absorption.
**Fig. 17.** Steepness-parameter estimation for SN 2008gz.

Please note: Wiley-Blackwell are not responsible for the content or functionality of any supporting materials supplied by the authors. Any queries (other than missing material) should be directed to the corresponding author for the article.

This paper has been typeset from a TEX/LATEX file prepared by the author.